Interaction of Snowmelt and Bedrock Permeability

Axel Keeß

Professur für Hydrologie der Albert-Ludwigs-Universität Freiburg i. Br.

Masterarbeit unter der Leitung von
Dr. Andreas Hartmann
Korreferent: Dr. Kerstin Stahl

Oktober 2015

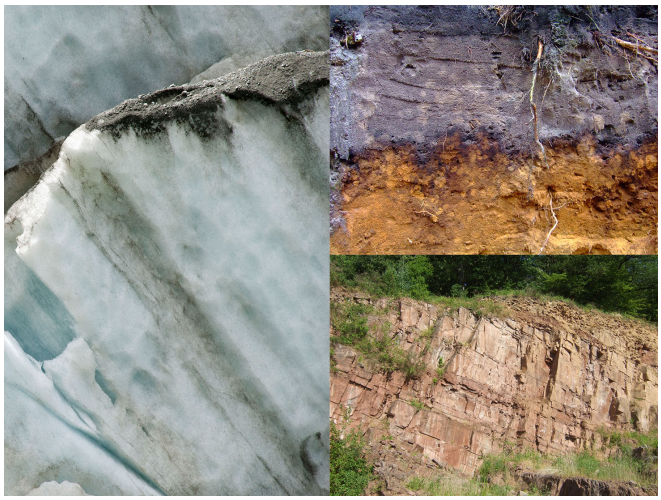

Contents

List of Tables

List of Figures

Nomenclature

CFMAX	Specific Maximum Degree-Day-Factor of Season
CFR	Refreezing Coefficient
CRHM	cold regions hydrological model
CWH	Water Holding Capacity
D	Darcy
DDF	Degree-Day-Factor
DEM	digital elevation model
DMS	Difference of Measured to Simulated Snowpack Days
EPOT	potential evapotranspiration
GIS	Geographic Information System
GLHYMPS	Global Hydrogeological Maps
HBV	Hydrologiska Byråns Vattenbalansavdelning
HRU	hydrological response unit
IQR	Inter Quartile Range
K	Hydraulic Conductivity
k	Bedrock Permeability
MAE	Mean Absolute Error
MC	Monte Carlo
MOPEX	Modell Parameter Estimation Experiment
MSD	Mean Signed Difference
NaN	Not a Number
NAS	Normalized Annual Streamflow
NCDC	National Climate Data Center
NOAA	National Oceanic and Atmospheric Administration
NOAA	National Oceanic and Atmospheric Administration
NRCS	Natural Resources Conservation Service
NSE	Nash-Sutcliffe-Efficiency

PGRADH	Fractional Precipitation Increase with Height
P	Precipitation
Q	Outflow
RC	Runoff Coefficient
RIR	Rain Infiltrated Ratio
ROS	Rain on Snow Factor
SAR	Snow Accounting Routine
SEM	Structural Equation Modeling
SF	Snow Factor
SIRI	Snowmelt Infiltration to Rain Infiltration
SIR	Snowmelt Infiltrated Ratio
SNOTEL	Snowpack Telemetry
SWE	Snow Water Equivalent
TLAPSE	Temperature Lapse Rate
T	Temperature
SFCF	Snowfall Correction Factor
TTSF	Temperature Threshold Snowfall
TT	Threshold Temperature
USDA	United States Department of Agriculture
USGS	United States Geological Survey

Abstract

The first part of this work describes a snowmelt modeling process on a daily basis for 78 snow-influenced catchments across the USA, all part of the MOPEX dataset. The dataset covers 53 years, from 1949 to 2001, the snowmelt modeling is based on a HBV-snow routine (degree-day-approach), adjusted to fit the wide variety of catchments: Season-dependent degree-day-factor, 250 m height zones and a rain-on-snow factor. The simulation shows that snowmelt intensities are generally lower than rain intensities, but differences exist depending on the progress and the duration of the melting period. In the second part of this thesis, infiltration rates of snowmelt and rain are determined and linked to streamflow data. The underlying assumption is that soils are saturated during snow melt, therefore hydraulic conductivity is the limiting factor for infiltration rates. Catchment wise mean hydraulic conductivity was calculated based on permeability information from the "global hydrogeological maps" (GLHYMPS) by Gleeson et al. (2014). By the help of linear regressions, results of this work show that in 43 of 78 catchments annual infiltration rates are correlated with annual streamflow, the majority of which (38) in a positive relation. Furthermore, in 33 catchments exists a significant correlation between a high snowmelt to rain ratio (in terms of infiltration composition) and streamflow. With these findings, current study partially confirms the findings by Berghuijs et al. (2014), who found a positive correlation between the annual snow factor of a catchment and its annual streamflow. These findings are of high importance in respect of climate change, as precipitation is very likely to shift from snow towards rain. With possible explanations for the work by Berghuijs et al. still lacking, current work tries to bridge this hydrological research gap.

Keywords

Snowmelt, Snow Routine, Infiltration, Hydraulic Conductivity, Bedrock Permeability, Degree-Day-Factor, HBV, Streamflow;

Kurzfassung

Im ersten Teil dieser Arbeit wird die Modellierung von Schneeschmelze auf täglicher Basis beschrieben. Diese wurde für 78 U.S.-amerikanische Einzugsgebiete aus dem MOPEX Datensatz durchgeführt und bezieht sich ausschließlich auf schneegeprägte Einzugsgebiete. Der Datensatz reicht von 1949 bis 2001 und umfasst somit 53 Jahre. Die Modellierung der Schneeschmelze basiert auf einer HBV-Schneeroutine, welche der hohen Diversität der Einzugsgebiete wegen noch weiter angepasst wurde: Ein saisonabhängiger Grad-Tag-Faktor, 250 m Höhezonen sowie ein Rain-on-Snow Faktor sind implementiert. Die Simulation zeigt, dass die Schneeschmelze generell ein geringeres Wasservolumen freisetzt, als ein durchschnittlicher Regentag mit sich bringt, Jedoch sind die Unterschiede zwischen den Einzugsgebieten sehr groß, was am individuellen Verlauf und der Dauer der Schmelzphase gezeigt werden kann. Der zweite Teil dieser Arbeit beschäftigt sich mit Infiltrationsraten und vergleicht diese mit jährlichen Abflussmengen. Dabei wurde die Annahme getroffen, dass lediglich das Festgestein eine Barriere für Wasser darstellt und die Böden gesättigt sind. Die hydraulische Leitfähigkeit wurde pro Einzugsgebiet aus der Permeabilität der oberflächennahen geologischen Schichten abgeleitet (GLHYMPS-Projekt von Gleeson et al. 2014). Es kann mit Hilfe linearer Regressionen gezeigt werden, dass für 43 der 78 Einzugsgebiete die jährlichen Infiltrationsraten einen Einfluss auf

den Abfluss haben. Außerdem wurde für 33 Einzugsgebiete ein linearer Zusammenhang zwischen einem hohen Anteil Schneeschmelze an der Gesamtinfiltration und hohen Abflüssen entdeckt. Mit diesen Erkenntnissen stützt vorliegende Arbeit in Teilen die Publikation von Berghuijs et al. (2014), in welcher ein positiver Zusammenhang zwischen einem hohen Schneeanteil am Gesamtniederschlag und dem jährlichen Abfluss festgestellt wurde. Hierfür gab es bislang noch keine Erklärung und doch ist die Thematik vor dem Hintergrund der Klimawandels brisant. Die vorliegende Arbeit soll einen Beitrag dazu leisten, die bestehende Forschungslücke zu schließen.

1 Introduction

1.1 Motivation

Climate change is of high rank in actual hydrological and especially snow-focused research. In a study about future snow cover and discharge in alpine catchments, Bavay et al. (2009) mention that "at altitudes below 1200 m a.s.l. a time-continuous winter snow cover is becoming an exception rather than the rule". According to them, "predicted changes in snow and discharge are extreme" and they even go as far as putting climate change on a level with downshifting elevation zones by 900 m. Less drastic but still intense, in a snowpack model sensitivity study on the ground of NOAA satellite dataset, Brown and Mote (2009) found out snow cover duration to be the most sensitive parameter in a warming climate of increasing temperatures and precipitation, varying with climate regime. To sum up these findings, Rasouli et al. (2014) examined the vulnerability of a Canadian mountain basin to change in temperature and precipitation through a physically based hydrological model: "The impact of 2 °C warming on snow could be fully compensated for by precipitation increasing by 20 %, but greater warming (>3 °C) cannot be compensated with precipitation increases of this magnitude" (p. 4202). As one can easily see from these findings, climate change is going to be of high influence to a very fragile and important part of the ecosystem and therefore resulting in socioeconomic implications: Taken the river Rhine as an example, Barnett et al. (2005) named "a reduction in water availability for industry, agriculture and domestic use during the season of peak demand" as a result of changes in the alpine head catchments.

But, how do changes in snow regimes affect water availability? This master thesis picks up from the findings of a previous study by Berghuijs, Woods and Hrachowitz (2014b) that came up with "A precipitation shift from snow towards rain leads to a decrease in stream flow". This was shown for a large number of catchments in the U.S., all part of the Model Parameter Estimation Experiment (MOPEX) described by Duan et al. (2006). Since an explanation for those findings is still lacking, this M.Sc. thesis investigates the coherence between snowmelt and infiltration capacity of the surface layer as a possible explanation. Gleeson et al. (2014) published a worldwide map about porosity and permeability of the earth's subsurface (GLHYMPS). Together with a Snow-Model which uses the MOPEX Dataset, snowmelt rates will be compared to hydraulic conductivities of the underlying bedrock under the assumption of saturated soils. The general idea hereby is, that snowmelt rates are generally lower than average rain rates and therefore less dependent on low hydraulic conductivities which depict a barrier for infiltrating water (fig. 1). With less water infiltrating, more water remains in the shallow subsurface or flows on the surface. In both cases it is strongly exposed to evaporation, resulting in a loss in the catchment's total water balance. This simplified model does not take the actual soil moisture into consideration, it assumes totally saturated soils or no present soil layer. Soil moisture rates are not part of the MOPEX data set, additionally the model was kept as simple as necessary in order to be able to complete the research in a given time of six months.

To sum it up, the general motivation for this thesis is to learn about the connection of snowmelt rates and the magnitude of bedrock conductivity. Additionally, a possible explanation or contradiction to the findings by Berghuijs, Woods and Hrachowitz (2014b) is intended. Another outcome of this study is to get a general idea about possible impacts of climate change on snow-affected catchments by the help of a 53-year dataset. Eventually, it is my personal motivation to learn more about

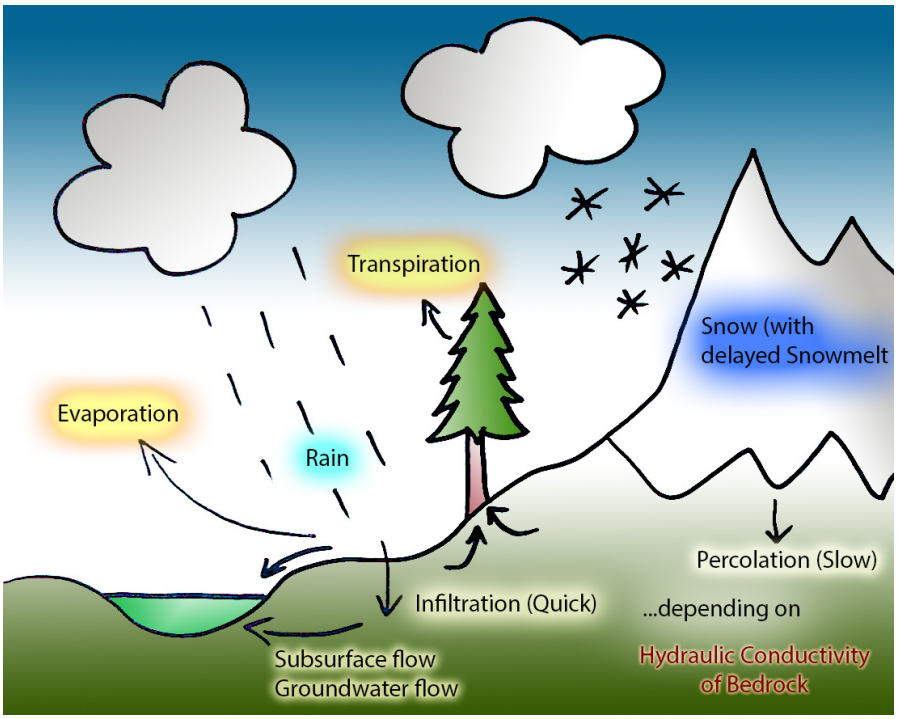

Figure 1: Simplified overview of hydrological flow processes: The figure shows that rain directly induces flow processes depending on intensity, infiltration rates and hydraulic conductivity of the underlying bedrock. In most cases snowfall leads to the formation of a snowpack with increasing extent over winter season. Snowmelt rates depend on different factors like snow density, air temperature and albedo of the snowpack, to name some of them.

hydrological processes on a large scale with an exceptionally extensive data set.

1.2 Short review on current state of research

In general, precipitation in form of snow delays flow-processes: In snow-affected catchments (snowfall $>$ 15 % of total precipitation, further referred to as snow factor SF) during average years, a snow pack is developed during winter, melting in spring- to summertime. High-mountainous areas (about 3000 m a.s.l. and higher) are usually snow-covered full season, resulting in permafrost soils but still contributing to discharge through a glacier's ablation zone. Polar region is not covered by any of the MOPEX catchments used in this study and therefore not further focused on. As presented in the "motivation" section of this thesis, there is enough scientific proof about upcoming changes resulting from climate change. As this thesis is about "snowmelt and bedrock conductivity", in the following a short review about the current state of research is given. The focus lies on the fields regarded to be most influencing for this thesis.

1.2.1 Snowmelt processes

In Pomeroy et al. (2006), the importance of snowmelt to streamflow is pointed out by the fact that snowmelt-processes supply 40 to 90 % of the annual streamflow. In a study on shrub tundra snowmelt, they found an average melt rate of 7 mm/d, depending on canopy. Pomeroy et al. (2006) further show that energy flow during melt processes under shrub canopies is still hard to quantify,

as there is no direct measuring method for sensible or latent heat fluxes. In terms of differences in snow melt between shrub and sparse tundra, Pomeroy et al. (p. 938) found “average shrub tundra melt rates being 47 % higher than that for sparse tundra”. This finding is induced by the higher snow accumulation of 147 % in shrub tundra.

A very fundamental and widespread approach into understanding of snowmelt and flow processes was done by Stottlemyer and Toczydlowski (1991) in "Stream chemistry and hydrologic pathways during snowmelt in a small watershed adjacent Lake Superior" as well as in "Seasonal change in precipitation, snowpack, snowmelt, soil water and streamwater chemistry, northern Michigan" (Stottlemyer and Toczydlowski 1999). Both works were carried out with extensive field monitoring effort and are therefore highly interesting in terms of this thesis. In "Stream chemistry and hydrologic pathways during snowmelt in a small watershed adjacent Lake Superior" (Stottlemyer and Toczydlowski 1991), airborne contaminants and their flow paths and travel times represent major research goals. Although the study is focused mainly on water chemistry, one can get a good insight into snowmelt processes. The study area, a 176-ha gauged catchment on the south shore of Lake Superior in Michigan, was intensely studied during winter of 1988 to 1989. The catchments mean elevation is 200 m a.s.l., peak snow-water-equivalent (SWE) was 260 mm in March of 1989. Continuous water sampling, lysimeter measurements, stream discharge and temperature measurements were carried out. Lysimeter outflow was measured with the help of tipping buckets. Groundwater tables were monitored with float gauges. Stottlemyer and Toczydlowski could show that despite of forming a permanent snowpack, forest soils would remain unfrozen and with snowmelt starting in January, “groundwater wells indicated most of this meltwater moved vertically through the forest soil”. During peak SWE, groundwater tables fell more than 700 mm, with estimated sublimation from the lysimeter plots of minor three percent. Intense increase of groundwater tables marked main snowmelt period from March to April, reaching soil surface in lower parts of the catchment. This lead to “extensive near-surface and overland flow” and the “greatest diurnal variation in streamwater discharge” (p. 185). Snowmelt rates during this period peaked at 8 mm per day. Stottlemyer and Toczydlowski concluded, that “the decline in groundwater height throughout winter until mid March indicated the increasingly important role of groundwater contributions to streamwater discharge up to the period of major snowmelt” (p. 193).

In their 1999’ publication Stottlemyer and Toczydlowski discussed the same catchment as in their former study, raising the data extent to one decade of monitoring with their focus on winter 1996-1997. Major hydrological insights of the study were that snowpack sublimation appeared to be < 15 % of precipitation input. Furthermore, diurnal patterns in groundwater levels following streamflow could be revealed, initiated by snowmelt with a time lag of 5 hours. This time lag would diminish with snowmelt reaching its peak. Stottlemyer and Toczydlowski also state that “evapotranspiration by tree foliation is of high importance for the annual watershed hydrologic budget” and “from mid-June to leaf fall, evapotranspiration was a major process limiting soil water recharge” (p. 2227). These findings underline the fragility of a snow-characterized catchment ecology, especially when one thinks about a possible future shift of snowmelt seasons.

In current research quite a lot of focus is given to the phenomenon of “Rain on Snow” (ROS) events. McCabe et al. (2007) examined a data set of 4318 sites in the western USA, finding that ROS events “are most frequent during the months of October through May” (p. 327). They also found

that ROS events vary on spatial patterns and follow temporal trends: with increasing site elevation, ROS events become more frequent. Further ROS examination was carried out by Freudiger et al. (2014), focusing on the major river basins in central Europe and the flood-generation potential of major ROS events. According to this study, for the Danube river ROS-generated runoff was an "average of 21, 28, and 35 % of the entire winter, early winter, and late winter precipitation" (p. 2702) in maximum years. The authors further state that "In a context of climate change, snowpack and precipitation in the wintertime are very likely to change and therefore may influence the frequency and magnitude of the flood hazard from rain-on-snow events in central Europe" (p. 2708). Freudiger et al. also underline the elevation dependence of ROS. They found some negative trends in ROS events from 1950-2011 probably being related with decreasing snowpack in late winter season. Still, ROS can have devastating consequences, as experienced during the ROS initiated flood from 2011 in Europe. A field study by Garvelmann et al. (2015) is the most recent contributor to ROS research: building up a network of 30 snow monitoring stations, a 40 km² mountainous catchment in southwestern Germany was examined. The authors were being able to record two major ROS flood events which occurred in December of 2012, deriving interesting understanding of the ongoing processes: "it is absolutely crucial for flood forecasting applications to know not only the basic snowpack information such as depth, density, and SWE but also its energetic state such as temperature and liquid water content". This statement was induced by the finding of the first ROS event being strongly buffered by a cold and deep snowpack with a high retention capacity for liquid water. With a more moist and warm snowpack at the second recorded ROS event, up to 60 % of total runoff was contributed through ROS.

1.2.2 Snow modeling

Hock (2003) provides an overview of temperature-index methods in their review paper "Temperature index melt modeling in mountain areas". She sees the biggest advantages of the degree-day method in their "good performance, low data requirement and simplicity" and predicts a "foremost position in snow and glacier melt modeling" (p. 112). By this, she confirms older statements from other authors, e.g. Rango and Martinec (1995) stating that the DDF method is "not easily replaced by more physically-based theoretical methods" (p. 668). However, the author states that limitations are found especially in the spatial and temporal resolution of the models, as mostly "average conditions" (e.g. temperature on daily basis, mean simulated snowpack for whole catchment) are observed. Hock also focuses on the Degree-Day-Factor (DDF) , as it has large influence on temperature-index models. A tabular overview of worldwide measured DDFs is given, clearly showing the wide range of values which it can be represented by. Referring to this wide range, Hock states: "Especially in mountain terrain, degree-day factors obtained from point measurements can generally not be assumed representative on the catchment scale" and "in degree-day driven run-off models, degree-day factors are more properly evaluated by optimization procedures (...)" (p. 112). Further focus on the DDF will be given in the "Methods" section of this thesis.

In 2007, Pomeroy et al. published a comprehensive study, trying to describe hydrological processes with physically based algorithms. The study is based on a field studies carried out in Yukon Territory, Northwest Territories and Saskatchewan, Canada. The authors linked the "physically-based algorithms (...) into a new modeling system that has resulted in the physically-based spatially-

Table 1: Number of catchments which were best simulated by each SAR. The SARs were combined with GR4J and HBV9 hydrological model. The HBV SAR is one of the best performing SARs, especially when combined with the HBV9 hydrological model. (Valéry et al. 2014)

	MOHYSE	CEQUeau	HBV	NAM	MORD4	M_SNE	CemaNeige	Total
GR4J	3	15	55	**107**	79	28	**93**	380
HBV9	6	46	**82**	52	67	49	**78**	380

distributed cold regions hydrological model (CRHM)" (p. 2651). CRHM works with so called "hydrological response units" (HRU), "spatial units of mass and energy balance calculation that correspond to biophysical landscape units" (p. 2651) in other words the modules for each aspect of the hydrological model such as soil moisture, snow drift or snowpack. Pomeroy et al.'s model is able to deal with factors which are especially found in Canadian catchments: extremely windy catchments with little vegetation would mean high exposure to blowing snow, a process which can be simulated via blowing snow HRU. Further processes represented in the model are: Snow redistribution, meltwater infiltration to frozen soils, runoff generation in alpine tundra and forest clearcuts. As one can see, CRHM is a very mighty tool, with good applicability in ungauged catchments without calibration. Pomeroy et al. engage other scientists to use CRHM as a modeling platform, making it freely available on the internet (http://www.usask.ca/hydrology/crhm.htm).

A very different approach is "As simple as possible but not simpler': What is useful in a temperature-based snow-accounting routine?", by Valéry et al. (2014). Examined is "the degree of complexity required in a snow accounting routine to ultimately simulate flows at the catchment outlet". The authors present the snow accounting routine (SAR) "Cemaneige" for simulating catchment outflow derived from snowmelt. It is based on different older SARs like HBV or MORD4 and tries to combine advantages between them. For validation, a set of 380 European and Canadian catchments was used. Most importantly, parameters which have no positive influence on model performance were not implemented. Valéry et al. first stated, that a subdivision of the catchments into single elevation zones is important and found 5 different height zones to be a good trade-off. An uneven snow-distribution with the height-zones was also found to be a parameter, which would increase the models performance and was therefore implemented. Furthermore, the authors found a slight improvement for their model when using a snowpack cold-content parameter in their SAR. When getting a season dependent melt factor in consideration, the authors found it not to be essential to their SAR but that it "could be useful on specific conditions or catchments" (p. 1182). Introduced by Bergström (1976), a water retention capacity parameter gives the SAR the possibility of holding back specific amounts of meltwater. Three major SARs use this approach, namely HBV, M_SNE and NAM. Still, Valéry et al. (2014) did not implement a retention capacity in their own model, due to lack of efficiency improvement. An overview of compared performances by different SARs in combination with two hydrological models can be seen in tab. 1. When concluding their work, Valéry et al. (2014) recommend to always start with a simple approach and step-wise addition of parameters when building up a SAR, to avoid unnecessary complexity in a model.

The most recent work on snowmelt modeling presented here will be "The value of multiple data set calibration versus model complexity for improving the performance of hydrological models in mountain catchments" by Finger et al. (2015). In their work, the authors present an enhanced version of the conceptual runoff model HBV-light in three levels of complexity. Calibration and val-

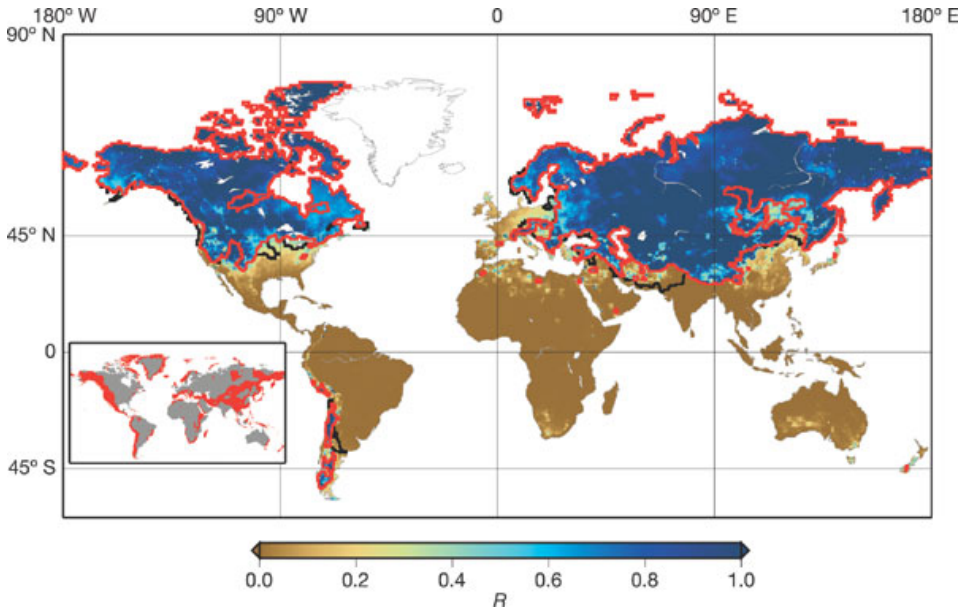

Figure 2: Illustration of the world's snow influenced areas: The unit "R" depicts the ratio of yearly snowfall to yearly recharge. The red surroundings are supposed to show areas with too little water storage capacity to buffer future losses due to shifting snowmelt periods. Figure by Barnett et al. (2005).

idation of simulations were realized using satellite-derived snow cover area and measured discharge values. The authors state that "increase in model complexity does not lead to a substantial improvement of modeling performance" (p. 1955), a similar statement as made by Valéry et al. (2014). More precise spoken, an implementation of aspect zones and vegetation zones into the model would not result in higher model performance.

Finger et al. (2015) could further demonstrate that 10k Monte Carlo (MC) runs with randomly generated parameters would produce 100 well performing parameter sets that could sufficiently simulate daily snow cover and discharge. When talking about calibration data, Finger et al. (2015) recommend to use different observational datasets, e.g. a combination of satellite-images with discharge data, additionally bringing a spatial component to the model. Snow-cover-images would also reduce a widespread problem with SARs, the frequent overestimation of snow-depths during summer months. Finger et al. (2015) conclude their paper as following: "Hence, in order to increase hydrological model performance, future efforts should focus on the acquisition, processing, publication, and incorporation of multiple data types into standard modeling procedures, rather than enhancing model complexity" (p. 1956).

1.2.3 Climate change and its influence on snow processes

Barnett et al. (2005) drew a rather severe picture of future water availability throughout large parts of the world, when reviewing studies on multiple fields regarding water processes. In fig. 2 one can get a good impression of how widespread future changes in climate will affect water resources on earth. One among them is the fact, that the peak of spring/summer snowmelt is going to be shifting one month earlier by 2050 (Barnett and Pennell 2004), an effect that bares further consequences: The later during wateryear main snowmelt is taking place, the higher is the potential evapotranspiration

(EPOT) and the water demand of the ecosystem. A shift would therefore be crucial for large parts of the ecosystem, depending on the current state of late snowmelt. The effect of earlier onsets of snowmelt seasons is confirmed by Stewart et al. (2005), caused by pacific decadal oszillation as well as a general warming trend. Barnett et al. (2005) show, that a decreasing snowpack is going alongside with decreasing water storage capacity: Like a glacier embodies a long-term water storage, winter snowpack is an important reservoir usually being emptied during seasons of high water demand. As shown by Singh and Bengtsson (2004), water from the Himalayan region supplies 60 % of the worlds population and is strongly depending on glaciers and snowmelt seasons. "The impact of climate change was found to be more prominent on seasonal rather than annual water availability" (p. 2363), with the crux that summer streamflow would usually contribute 60 % of total year's streamflow. Stahl et al. (2006) cold show for British Columbia, Canada, that glacier melt is contributing less to August streamflow, concluding that the research area "already passed the initial phase of warming-induced increased runoff" (p. 5). Further examined by Nolin et al. (2010) this could be quantified: "(...) Eliot Glacier discharge increases 13 % for every 1°C increase, but decreases 9 % for every 10 % decrease in glacier area" (p. 12).

Barnett et al. (2005) brings up the aerosol-related problems, especially black carbon is able to lower the albedo of snow and ice masses and will enforce the problem of earlier snowmelt seasons and smaller snowpacks.

Campbell et al. (2010) refer to a former postulated paradox by Isard and Schaetzl (1998), after which a warmer world could lead to colder soils as an effect of decreasing snowpack insulation of soils. They state, that there are only "negligible changes in maximum annual frost depth over the past half century" (Campbell et al. 2010, p. 2478) as concluding of a long term data set of Hubbard Brook Experimental Forest, New Hampshire, USA. Their further appliance of a soil energy and water balance model suggested only little change in soil frost depths over the period from 2009 to 2099. Interestingly, "although climate model projections for the Hubbard Brook Experimental Forest suggest that winter precipitation will increase during the 21st century, there has been no evidence for such a trend over the past half century" (Campbell et al. 2010, p. 2478) , implying that with no significant rise in precipitation rates, snowpack decrease will be by far worse than usually expected. In general this shows, how important reliable long term field studies are for the verification of climate models.

1.2.4 Influence of the soil bedrock barrier on groundwater recharge

Gburek and Folmar (1999) carried out a groundwater recharge field study in the Susquehanna River Basin in Pennsylvania, an area also covered by a MOPEX site. A core drilling of 30 m depth allowed a characterization of the bedrock as sandy shale, siltstone and sandstone. The profile was found to be highly fractured over the entire depth. Hydraulic conductivity K was found to be 1300 mm/d inside the highly fractured, and 400 to 500 mm/d inside the moderately fractured layers. A K-value that was found for a poorly fractured site was 200 mm/d. Gburek and Folmar (1999) were further able to demonstrate that percolating water amounts were directly induced by precipitation and snowmelt. Growing season resulted in less percolation at similar rain amounts. A time lag of 1-2 hours between start of percolation and groundwater response could be measured.

Macpherson and Sophocleous (2004) studied a floodplain aquifer in northeast Kansas over two

and a half years. Interestingly, they did not find vertical pathways through bedrock to be the primary process of recharge: Limestone fractures of surrounding bedrock represented a preferential flow path, whereas average K values of the floodplain aquifers were low.

Rodhe and Bockgård (2006) examined groundwater response to rainfall and snowmelt in a fractured rock aquifer in Sweden. Most importantly hereby was the finding, that although covered by 10 m thick till soils, groundwater level would quickly respond to precipitation events. By the help of a simple model-approach, Rodhe and Bockgård (2006) were further able to proof their hypothesis of groundwater being "fed by local recharge from the overlying soil aquifer" (p. 389).

A study by Gleeson et al. (2009) was driven by the fact that recharge processes involving fractured rock aquifers covered with a soil layer are poorly understood. The hydrogeological subsurface of their research area in Tay River watershed in Eastern Ontario, Canada, was found to be highly heterogeneous. Gleeson et al. (2009) found rapid recharge due to vertical bedrock fractures to be the dominating process in their research area. According to them, the "hydrogeomorphic setting (of humid fractured soils) is common in Canada, the northeastern United States and northern Europe" (p. 507).

Voeckler and Allen (2012) estimated K values of regional fractured aquifers in the mountainous Okanagan Basin, British Columbia, Canada. Their approach included mapping of discrete fractures from outcrops and orthophotos and a simulated pumping test. "A paucity of groundwater data in mountainous environments worldwide due to a lack of wells in these high elevation settings" (Voeckler and Allen 2012, p. 1081) is the authors main incentive hereby. K-values resulting from their study are 0.9 - 9 mm/d, being about 3 times higher in areas with greater influence of larger-scale fractures. By the help of these findings, Voeckler and Allen (2012) were able to approve K values by Gleeson et al. (2011), which build the basis of current thesis.

Ostendorf et al. (2015) carried out a field study in Eastern Massachusetts, USA. They focused on a glacial till drumlin called Scituate Hill, with weathered brown till on top of an unconfined aquifer. The study showed that a K-value of 0.4 mm/d for the glacial till limited percolation into the aquifer. Water table was found to "vary sinusoidally with a 1.3 m amplitude" (p. 755), with 30 % of the average recharge coming from a gray till aquitard beneath the drumlin. Ostendorf et al. (2015) found the drumlin to be homogeneous and tight with a total porosity of 0.2 due to calibrated pumping.

1.2.5 Research Gap

As seen in the previous section, climatic influences on past and future water availability are widespread and not totally understood up to this point. And there are many other areas in the need of further research. Berghuijs, Woods and Hrachowitz (2014b) brought more confusion into the discussion, when stating that "a precipitation shift from snow towards rain leads to a decrease in streamflow". But how did they get to publishing this statement?

Berghuijs, Woods and Hrachowitz (2014b) concluded a statistical analysis of the MOPEX dataset, containing recharge data of 420 catchments spread over the whole USA. When applying the Budyko water balance framework, a method to make different catchments of various climatic settings being comparable by using the ratio of mean potential evaporation to the mean precipitation, they found out that "larger values of snow factor (SF) are associated with lower normalized evaporation (...) and

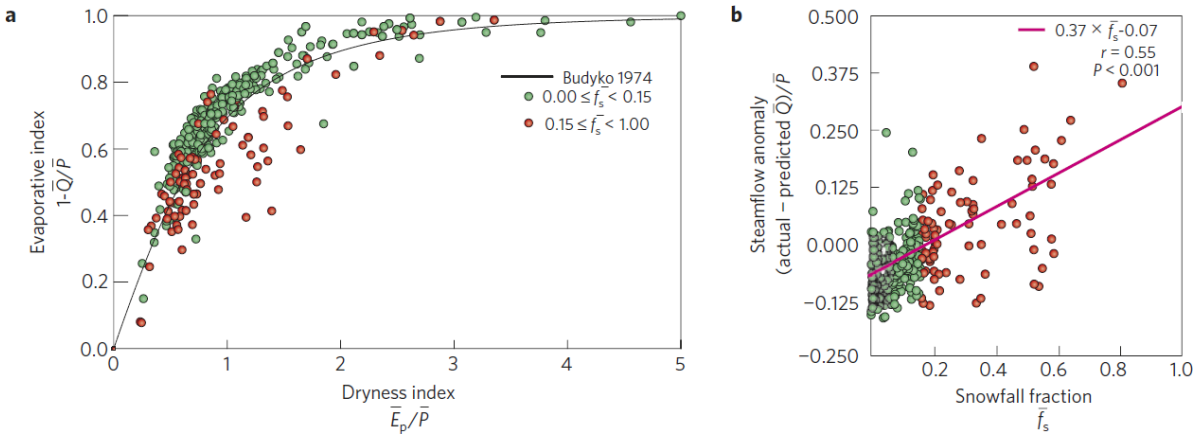

Figure 3: Mean annual streamflow and streamflow anomaly in the context of the Budyko hypothesis, stratified by snow fraction**:** The observed long-term streamflow and precipitation measurements are placed in the context of the Budyko hypothesis. The Budyko hypothesis states the mean streamflow is primarily a function of the catchment's annual precipitation and potential evaporation as shown by the black line in a. Departures below the Budyko curve for catchments with a significant fraction of the precipitation falling as snow indicate that an increased fraction of precipitation as snowfall is associated with higher streamflow, as clarified by the linear regression in b. (Figure and description by Berghuijs, Woods and Hrachowitz 2014b)

higher normalized mean streamflow" (fig. 3) . The next step by Berghuijs, Woods and Hrachowitz (2014b) was to take a closer look on all catchments with a SF of at least 15 %, resulting in 97 catchments remaining. With the help of linear regressions they tried to find a linkage between the normalized annual streamflow $Q/\overline{P}$ and the SF. The mean increase of $Q/\overline{P}$ per unit of SF was found to be 0.29 (standard deviation 0.21) and 94 of the 97 catchments showed a positive value of this sensitivity. Fig. 4 shows the sensitivity of normalized annual streamflow to annual SF for the 97 catchments. Sensitivity is defined as the change in normalized annual streamflow $Q/\overline{P}$ per change in the annual SF. For the authors, "the observation that a lower SF is associated with lower streamflow on the annual and mean-annual timescales is restricted here to empirical evidence, and does not reveal the physical processes behind these observations". Berghuijs, Woods and Hrachowitz give multiple factors influencing the sensitivity of streamflow changes:

- differences in water storage dynamics
- flow paths and evaporation due to changes in the infiltration capacity of soils
- the duration of infiltration periods
- the timing of infiltration periods
- the evaporation from snow-covered and snow-free soils
- the growing season length
- the soil moisture regime
- the potential evaporation

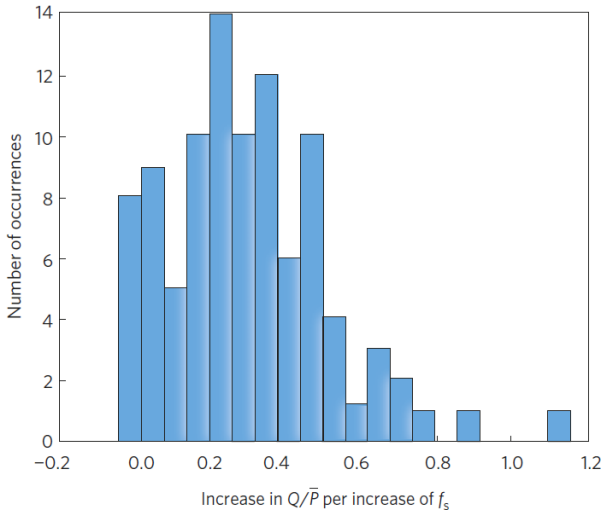

Figure 4: Sensitivity of annual streamflow to the fraction of annual precipitation falling as snowfall**:** The histogram shows the change in normalized streamflow $Q/\overline{P}$ per unit change of the SF. Positive values of sensitivity indicate that the annual streamflow of catchments varies (between years) directly with the annual SF. Years with higher SF tend to have higher values of annual streamflow. (Berghuijs, Woods and Hrachowitz 2014b)

There is a clear research assignment in the lacking explanation for the findings by Berghuijs, Woods and Hrachowitz (2014b), intensified by the ongoing changes in climate behavior, the effect of altered snowmelt processes and their consequences for future water availability. Groundwater recharge is strongly depending on bedrock, but hydraulic conductivities are hard to determine due to high heterogeneity of the near-surface layers. Gleeson et al. (2014) tried to gather all available information and published the "global hydrogeological map". Together with the MOPEX dataset, there is enough data at hand for research on the large scale interaction of snowmelt and bedrock permeability.

1.3 Problem and ambition

In this work, the connection between bedrock permeability and infiltration rates is of primary interest. The MOPEX data set only contains precipitation information for the water year, there is no fraction into rain and snow. Therefore, rain needs to be separated from snow. In the following, a snow routine capable of simulating the snowpack's development and melt must be built. Hereby, an appropriate model approach and choices between model complexity and efficiency have to be made. In this question, respect is given to the recent work by Valéry et al. (2014). As the MOPEX catchments are geographically widespread, difficulties with adjusting the snow model's parameters are to be expected. In order to make them "best fit" for every catchment, a trade-off between applicability on a large scale and precision on catchment layer is needed. Another question is, if model calibration is possible. If yes, are individual parameter values on catchment layer or a full size calibration approach the correct answer? The DDF is hard to determine (Hock 2003) but one of the most essential parameters in our snow model. It needs special consideration therefore.

Based on the described problems, the snow model is intended to simulate snowmelt rates on a daily basis. The model's uncertainty must be known, in order to analyze the link between snowmelt

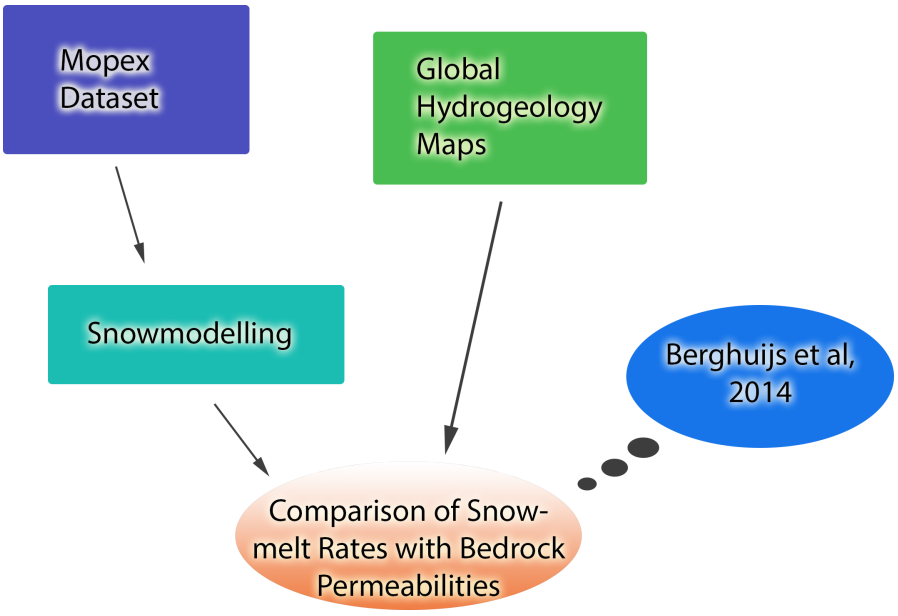

Figure 5: Flow chart of research design: The MOPEX dataset as well as the "global hydrogeology map" mark the starting products. Snowmelt will be modeled on a daily basis through the help of a self-programmed snow accounting routine. Finally, assertions towards snowmelt rates, their comparison with rain rates and the infiltration capacity depending on the hydraulic conductivity of the bedrock will be made. By the help of this, we hope to be able to conclude to the findings by Berghuijs, Sivapalan, Woods and Savenije (2014).

rates and bedrock conductivity. As the GLHYMPS has it's own uncertainty, this factor must be taken into consideration as well. Outgoing from this results, it may be possible to show if or if not low bedrock permeability represents a barrier for infiltrating water and if snowmelt rates make a difference compared with rain events. Finally, if there is a link between those two, can the results be seen in the catchment's streamflow? And subsequently, is it possible to give an explanation to the findings by Berghuijs, Woods and Hrachowitz (2014b), which stated that "a precipitation shift from snow towards rain leads to a decrease in streamflow". A simplified overview of this thesis's approach and ambition can be seen in fig. 5.

The questions that are to be answered in this thesis are:

- What can be learned about snowmelt rates from our simulation?
- Are daily snowmelt rates generally lower than daily rain rates?
- Do bedrock hydraulic conductivities represent a barrier for infiltrating water?
- Is there a correlation between infiltration rates (snowmelt, rain) and streamflow?
- Do these results support the Berghuijs, Sivapalan, Woods and Savenije 2014 study or do they imply a conflict?

2 Methods

2.1 Software and hardware overview

All data processing as well as the implementation of the snow model was realized in MATLAB (version R2015a). All documented code files are supplied on the attached DVD and are described in their functionality in tables A.1, A.2 and A.3 of the appendix. As geographic information system (GIS), ArcGIS (version 10.2.2) was deployed. Further software used for this master thesis were HBV (version 3.0.0.1), mostly for control purposes, and the use of the HBV-help as well as Photoshop (version CS6) for image processing. A Dell Latitude E4310 with an Intel Core i5 (2.8 GHz), 4 GB of RAM and an 128 GB SSD acted as hardware basis.

2.2 Data basis and preparation

The input data of this thesis will be described in this section. An overview of the data can be seen in following tab. 2:

Table 2: Input Data Overview

Input Data	Data Type	Source
MOPEX	.txt	ftp://hydrology.nws.noaa.gov/pub/gcip/mopex/US_Data/
GLHYMPS	.gdb	courtesy of Gleeson et al.
SNOTEL	.txt	http://www.wcc.nrcs.usda.gov/snow/
USA DEM (digital elevation model)	.adf	http://hydrosheds.cr.usgs.gov/dataavail.php

2.2.1 MOPEX data set

The freely available MOPEX data set depicts the data basis for this study. It is further described by Schaake et al. (2006) and includes:

MOPEX dataset overview

- 438 Catchments in the USA (with areas from 67 to 10000 km²) in all climate zones except polar climate of which 97 are snow-affected (SF > 0.15) (see fig. 6)
- 24-hour precipitation data [mm]
- Daily outflow data Q [cubic feet per second], potential evaporation [mm], max and min air temperature [°C]
- Climatic potential evaporation (mm/d) (based on National Oceanic and Atmospheric Administration (NOAA) Evaporation Atlas)
- Well-described additional information to each catchment (soils, vegetation, greenness etc.)

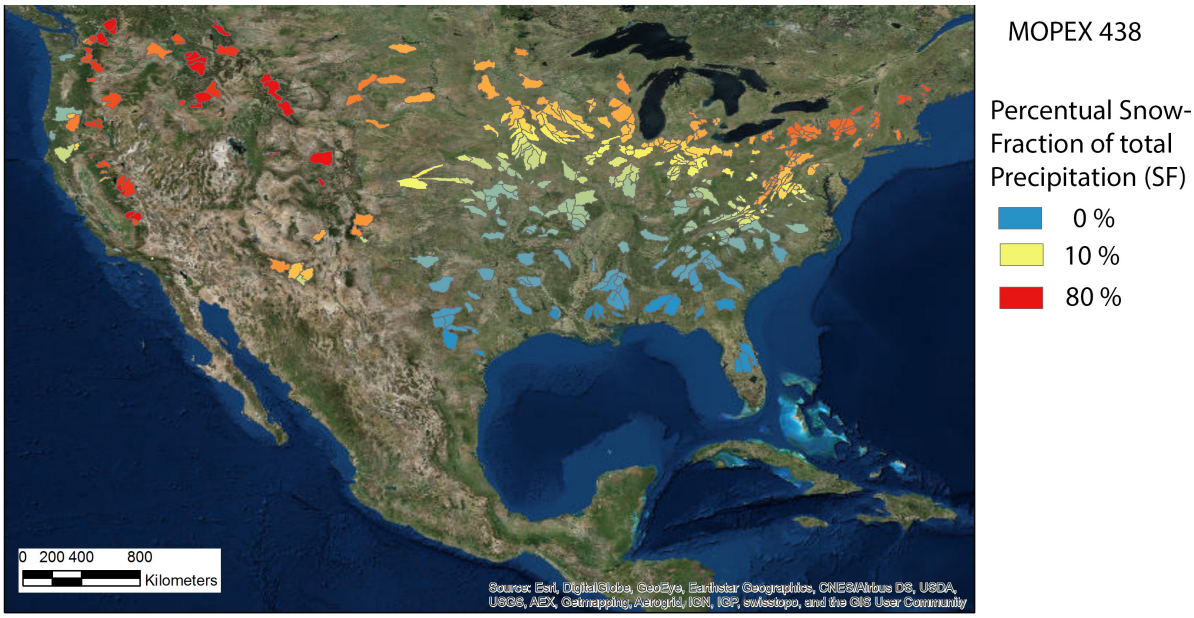

Figure 6: Overview of all 438 MOPEX catchments and their snow factor: The map clearly shows that large areas are not or only weakly affected by snow. We only used catchments with a SF $>$ 15 % for this thesis, therefore all catchments marked in shades of yellow to blue are not being considered.

When starting to work with the data set, various adaptions had to be made. All non-metric units were transformed into metric units (e.g. cubic feet into liters). T, P and Q data sets had different start- and end-dates, therefore they had to be trimmed to the correct time frame with hydrological year starting on 1st of October. This makes a total of 53 years of continuous data. A routine to deal with missing values was established in MATLAB, deleting catchments with less than 15 years of data and standardizing missing values to the MATLAB standard "NaN" (Not a Number). This step affected 17 catchments.

Next, catchments with a SF smaller than 15 % were taken out of the dataset, according to Berghuijs, Woods and Hrachowitz (2014b). As the relation of snowmelt on bedrock conductivity is about to be demonstrated, catchments with less snow influence than 15 % are not considered to be representative. This step reduced the dataset from 421 to 98 catchments. When looking on the catchments in ArcGIS, several catchments were found to be "nested", meaning one catchment would directly contribute to the outflow of another one. As this could result in a bias, it was determined to get rid of any nested catchments. This step was undertaken in ArcGIS and the dataset was limited from 98 to 78 snow-influenced and non-nested catchments finally.

An overview of the MATLAB routines dealing with data preparation can be seen in table A.1 of the appendix.

2.2.2 "GLobal HYdrogeology MaPS" (GLHYMPS)

The "GLobal HYdrogeology MaPS" (GLHYMPS) of permeability and porosity (Gleeson et al. 2011, 2014) is a worldwide lithology map with an average raster solution of 100 km². Respectively

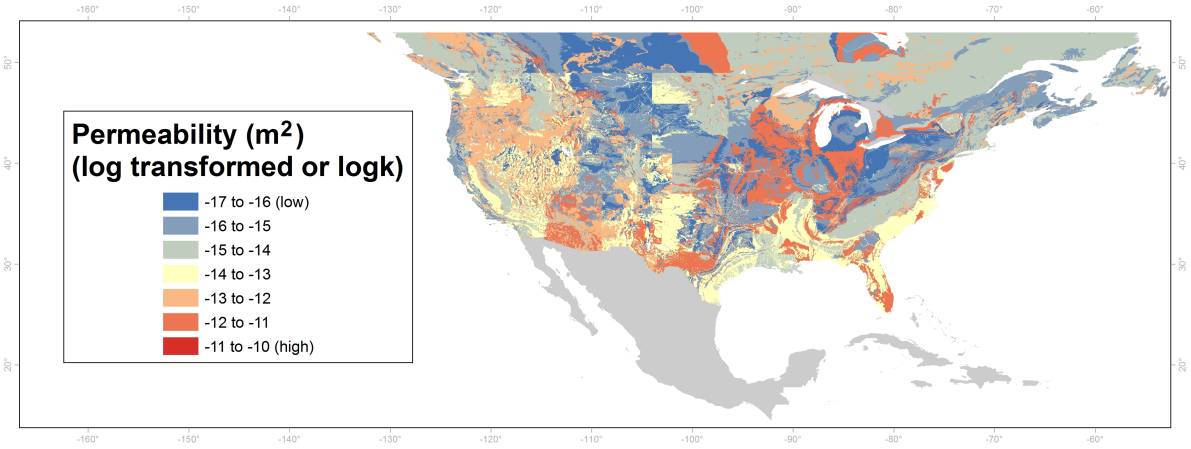

Figure 7: "GLobal HYdrogeology MaPS" (GLHYMPS) of permeability and porosity**:** Permeability is displayed in the unit of m². The values represented by the colors are on a logarithmic scale. As most geological surveys are used to different classifications used for bedrock permeability, artifacts like the one on the Canadian-American border are a result. Figure by Gleeson et al. (2014)

for U.S., the resolution of the map is much higher (fig. 7). It includes the bedrock permeability k in m² on a logarithmic scale as well as the bedrock porosity. Additionally, a value for the standard deviation is given to each of the two quantities. The term "permeability" originally comes from the field of oil petrology, describing the nature of a rock's pore system independent of the fluid viscosity (Hölting and Coldewey 2009), measured in the unit Darcy (D) or m². In the field of hydrology, the unit [m/s] or [mm/d] is used with the hydraulic conductivity K. Both coefficients can be converted to each other by the help of equation 1 (Hölting and Coldewey 2009):

Conversion of permeability k into hydraulic conductivity K:

$$K = k * \frac{g * \rho}{\eta} \tag{1}$$

with

K = hydraulic conductivity [m/s]
k = bedrock permeability [m²]
g = local gravity [m/s²], = 9,81 m/s²
ρ = density [kg/m³], water = 999.97 kg/m³
η = viscosity [Pa*s], water = 0.001 Pa s

The GLHYMPS was kindly provided by Tom Gleeson in form of a GIS-geodatabase. The conversion of the original data into K was done in ArcGIS field calculator, as well as the conversion of the standard deviation. Both values (logarithmized and multiplied by 100) are originally stored as integers in the GLHYMPS-geodatabase, as this datatype needs less storage space than a float value. After the conversion, with both entities in the unit [mm/d], a plot of the distribution of the conductivities was done, to get a good impression of how the catchments mean-conductivity should be calculated (fig. 8).

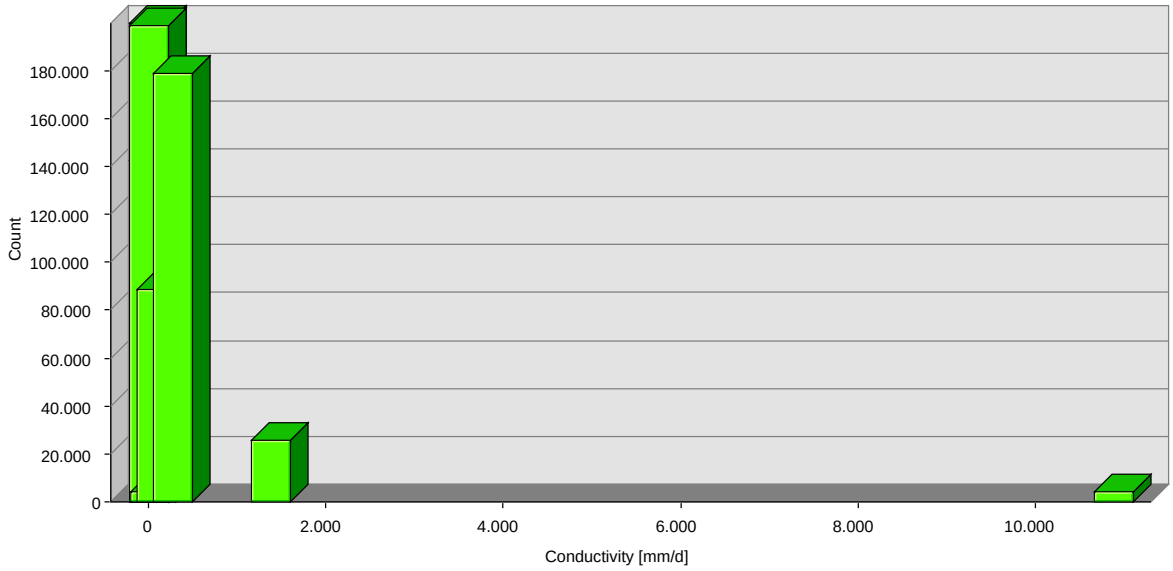

Figure 8: Distribution of hydraulic conductivities part of the MOPEX catchments : The data's distribution is of high skewness, with the majority of values between 0 and 250 mm per day (the bars are displayed thicker for better visibility). A small fraction in terms of surface area is of extremely high conductivity values of ca. 11000 mm/d.

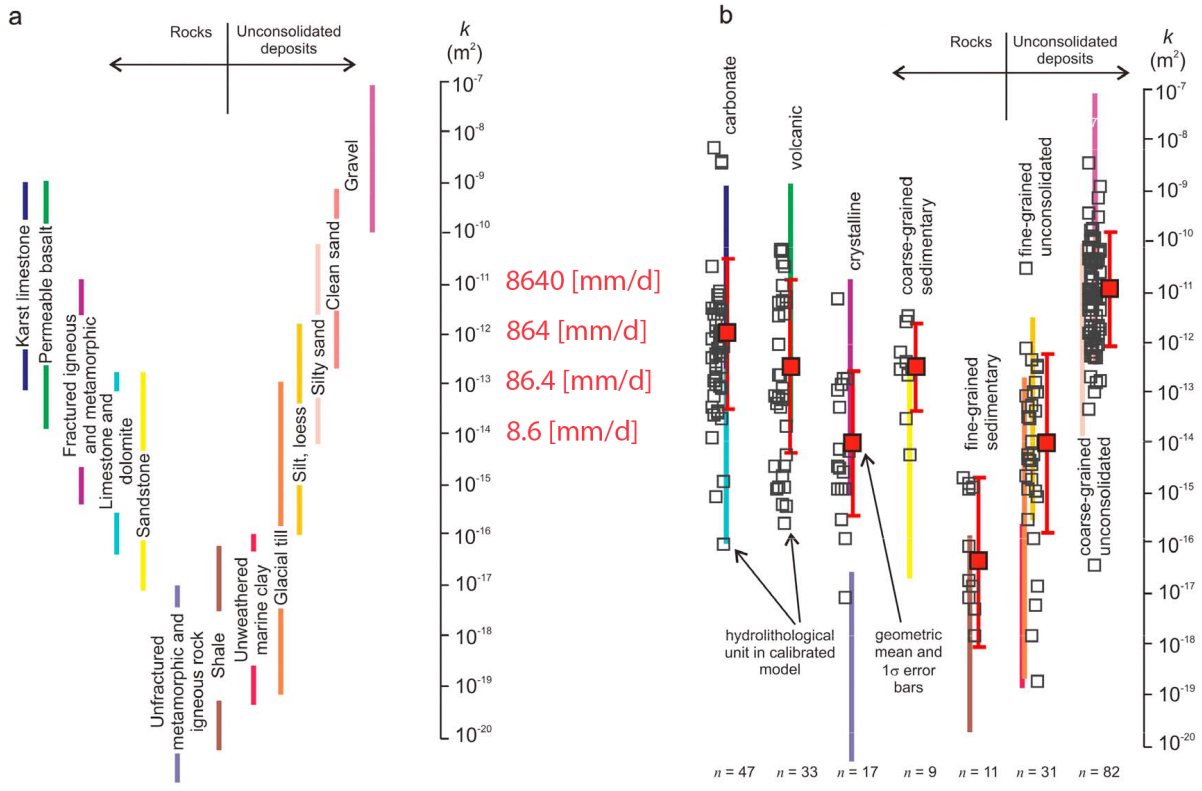

Figure 9: Overview of bedrock permeability determination: Figure a) shows the wide span of each class and the huge range of permeability values. The large red numbers between a) and b) represent the corresponding K value. In b), local scale permeability ranges are shown behind the open squares by the same colored bars. Values are grouped into hydrolithologic categories (i.e., fine grained unconsolidated). The red dots symbolize the mean value (geometric mean) for a category, with the standard deviation represented through red lines. Figure originally by Gleeson et al. (2011). The red numbers in the middle were added later.

The extreme skewness of the distribution of conductivity values in our 78 catchments is most probably based on huge differences in bedrock geology, on which the map by Gleeson et al. is based. In fig. 9, it gets clear why K derived from permeability (fig. 8) is so unequally distributed: When establishing the GLHYMPS, Gleeson et al. had to categorize the bedrock into hydrolithological units. With a huge variety of permeability values for each category, often spanning over more than 3 powers, they found those to be best represented by the geometric mean (see also Zinn and Harvey 2003). As a consequence, standard deviation values are pretty high and are therefore going to be further considered in this thesis. Furthermore, e.g. the step between carbonate rocks and gravel (the two most permeable categories) represents an increase of the factor 10 regarding permeability. For this study, it was determined to build the catchment-wide mean conductivity through the geometrical mean, as seen in Gleeson et al. (2011). The arithmetic mean is not robust against outliers and produces comparatively high conductivity values. For the computation of the geometrical mean, the ArcGIS-command "tabulate intersection" was used, which produces percentage information about the K- categories of a catchment and their standard deviation. This table was exported to MATLAB, where the geometrical mean as well as the resulting standard deviation was calculated. For the resulting standard deviation, equation 2 was used:

Propagation of uncertainty with $f(p_i)$ = any function

$$\sigma_{f(p_i)} = \sqrt{\left(\frac{\partial f(p_i)}{\partial p_1}\right)^2 \sigma_{p_1}^2 + \left(\frac{\partial f(p_i)}{\partial p_2}\right)^2 \sigma_{p_2}^2 + \ldots + \left(\frac{\partial f p_i}{\partial p_n}\right)^2 \sigma_{p_n}^2} \tag{2}$$

A barplot and boxplot of the resulting K and its standard deviation is shown in fig. 10. According to the whiskers of the boxplot, 90 % of all values range between 0 and 15 mm/d, the standard deviation is approximately a quarter of the geometric mean but varying strongly. When taking a look at the geographic distribution of K between the 78 MOPEX catchments (fig. 11), no major patterns are visible, if any, there is an aggregation of low conductivities in the catchments between the states of Pennsylvania and New York.

In fig. A.1 and fig. A.2 of the appendix, bedrock geology and resulting hydraulic conductivity are depicted for Susquehanna River catchment between the states of Pennsylvania and New York. The need of a robust mean approach is underlined hereby, as conductivity values are very uneven distributed in this catchment.

2.3 Snow Model

After learning about different approaches of snow modeling (Hock 2003, Pellicciotti et al. 2005, Stahl et al. 2008, Valéry et al. 2014), it was determined to use a modified standard HBV-Snow-Routine (Bergström 1976, Seibert 1997), which is basically explained in the box of section 2.3. HBV was chosen due to the fact of its good performance (Valéry et al. 2014), wide applicability and simple structure. Aside from that, HBV has a long history in hydrological modeling (Bergström 1976) and has continuously been improved (Lindström and Bergstöm 1992, Seibert 1997). Additionally to the HBV SAR, we used a 250 m height-zone stepping, as it is recommended by Valéry et al. (2014) to use

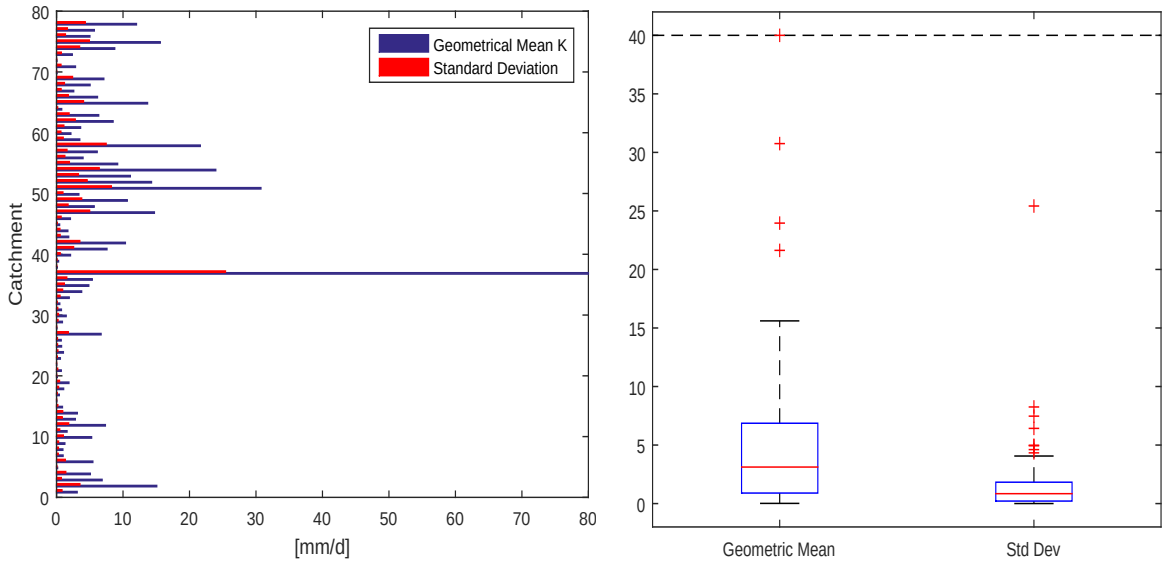

Figure 10: Overview of hydraulic conductivity K and its standard deviation: The left hand figure shows the mean K value for each catchment with a blue and the according standard deviation with a red bar. On the right hand side, a boxplot highlights the distribution of the values (box: red line = median, box limits = quantiles, whiskers = 1.5 * box size)

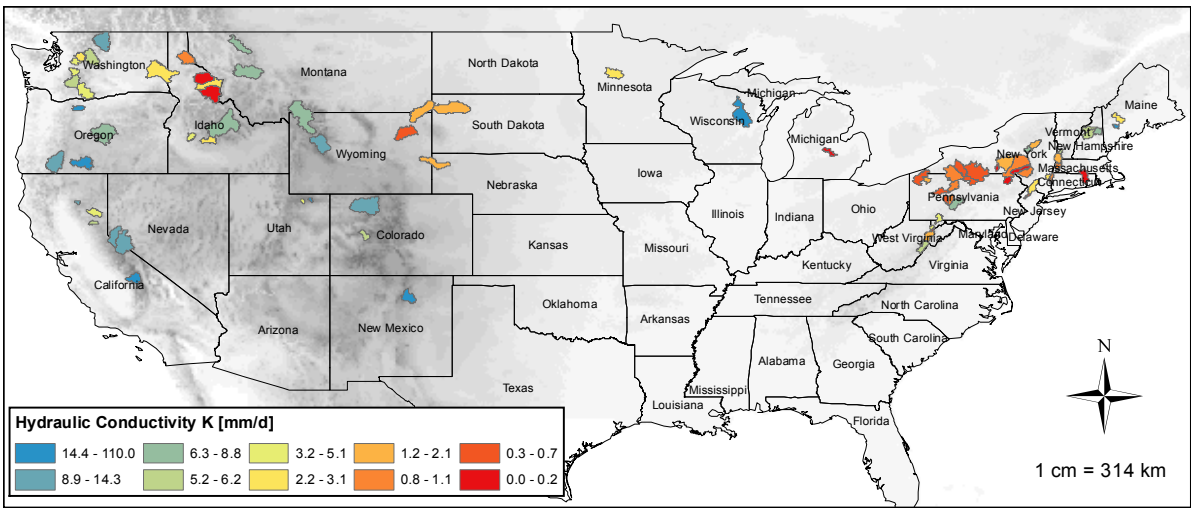

Figure 11: Overview of mean hydraulic conductivity K in 78 MOPEX catchments: The computed geometric mean values are displayed, with no general pattern visible. Catchments lying next to each other often share the same or a close value which can be attributed to regional geology.

different height zones in a SAR. For height zone classification, a 15-arcsec-DEM of the United States was downloaded from USGS' Hydrosheds-website (Hydrosheds DEM). In ArcGIS, we used the "calculate statistics tool" and afterwards the "reclassify" command. Finally, the command "tabulate area" was used to produce a table with a fractional value for each height zone respective to the total area.

Snow Routine Overview (HBV Manual, Seibert (2010))

Input Data:

- Precipitation (P), Temperature (T)

Output Data:

- Snow pack, Snowmelt

Parameters:

- TT = Temperature Threshold (° C)
- DDF = degree-day factor [mm $°C^{-1}$ d^{-1}]
- CFMAX = specific maximum degree-day-factor of season [mm $°C^{-1}$ d^{-1}]. Only further referred to in MATLAB snowroutine.
- SFCF = snowfall correction factor [-]
- CFR = refreezing coefficient [-]
- CWH = water holding capacity [-]

General Routine Description

1. Accumulation of precipitation as snow if the temperature is below TT
2. Melt of snow starts if temperatures are above TT calculated with a simple degree-day method
3. Meltwater = CFMAX (T-TT) [mmd^{-1}]
4. CFMAX varies normally between 1.5 and 4 mm °C/d (in Sweden), with lower values for forested areas. As approximation the values 2 and 3.5 can be used for CFMAX in forested and open landscape respectively.
5. The snow pack retains melt water until the amount exceeds a certain portion (CWH, usually 0.1) of the water equivalent of the snow pack. When temperatures decrease below TT this melt water refreezes again.
6. refreezing meltwater = CFR·CFMAX (TT-T)

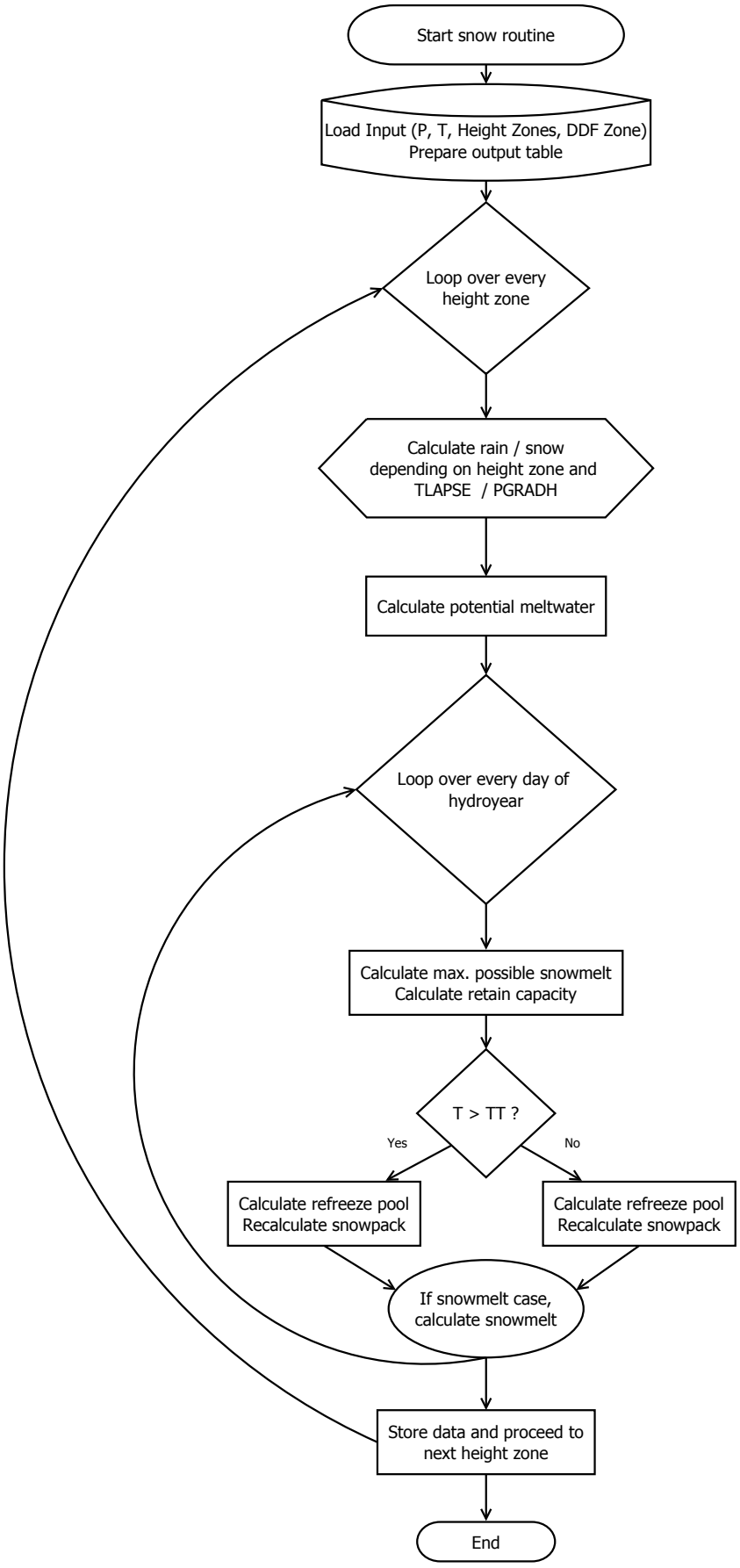

Figure 12: Flowchart of the snow routine: Processes are depicted simplified, the general understanding of the involved steps is of primary interest.

Figure 13: Picture of an example SNOTEL site: Air temperature is measured via shielded thermistor (left), precipitation via storage type gauge (middle). Snow water content is measured by a snow pillow device and a pressure transducer (not visible). Snow depth is measured with a sonic sensor (in the background). Picture by NRCS (http://www.wcc.nrcs.usda.gov/snow/).

2.3.1 Parameter estimation

A general approach for the development of a snow model would be to conclude a sensitivity analysis, which would require reference data to our simulated snowpack SWE for all catchments. It was not possible to get SWE data to all 78 catchments, we only came across with 8 catchments and a total of 18 years of SWE. Therefore we decided to leave out the sensitivity analysis, and carry out a calibration for the parameters which can't be specified by literature values. The SWE measured references were taken from the freely available SNOTEL project's dataset. SNOTEL stands for automated SNOwpack TELemetry and maintains weather stations in 13 Western U.S. states. It is run by the United States Department of Agriculture (USDA) Natural Resources Conservation Service (NRCS) . SNOTEL is understood to be a "formal cooperative Snow Survey and Water Supply Forecasting (SS-WSF) Program" (NRCS 2008). Some of the SNOTEL stations supply SWE data since the 1960's, but most data is available since the late 1980's. SNOTEL sites use satellite burst communication for a wireless data transmission, the stations have usually only to be maintained once per year. SWE is measured by a snow pillow device and a pressure transducer USDA (2014).

A picture of a standard SNOTEL site can be seen in fig. 13. Eight SNOTEL stations could be matched to MOPEX catchments, most of them lying inside a MOPEX catchment or very close. As the snowmodel calculates SWE values for different height zones, these could be used to calculate a mean value between the two height zones under and above the SNOTEL station. 18 years of SNOTEL data (1984 to 2001) could be used. An overview of the SNOTEL Stations and their related catchments can be seen in Table 5 on page 37. Fig. 15 shows the position of the catchments

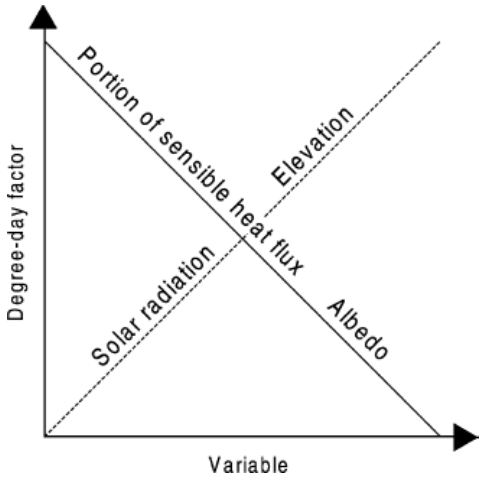

Figure 14: Influences on the Degree-Day-Factor: The DDF increases with rising solar radiation and elevation, and decreases with rising portion of sensible heat flux and albedo. Figure from Hock (2003)

which could be matched with a SNOTEL station.

Snowpack and snowmelt are strongly depending on the DDF, which is hard to determine and is roughly ranging between 1 and 8 [mm $°C^{-1}$ d^{-1}] (Hock 2003). As a result of the high influence on the snow model's efficiency, we decided to keeping neither one single DDF for all catchments, nor a specific for each catchment. A middle course had to be found. Most influencing factors on the DDF are shown in fig. 14. As the DDF is strongly depending on elevation and latitude of the catchment, we decided to build 3 clusters of catchments, according to their geographic position and their topography. Slope and mean height of the catchment as well as information on the latitude were already provided through pre-processing of GIS data. A "k-means"-approach was used to group the 78 catchments with individual slope, height and latitude into 3 clusters. Cluster analysis with k-means is also known from different studies (Hartmann et al. 2015). The general functioning of k-means is to compute sum distances between all potential cluster values and group the ones with similar distance. When using k-means, one has to decide how many clusters he wants to use. When using the k-means function in MATLAB, there is an option to plot the mean sum-distances of a range of clusters, making it easy to determine when the best number is reached. The accompanying code is found in the script "Categorize_Catchments.m". In our case, 3 clusters were the optimum. Finally, we decided to calibrate each DDF in a specific range for each cluster, as can be seen below:

DDF cluster overview

1. Cluster: Low Mean Elevation and Slope, High Latitude -> rather low DDF, range of [2 ... 2.5] [mm $°C^{-1}$ d^{-1}]
2. Cluster: Mid Mean Elevation and Slope, Mean Latitude -> rather medium DDF, range of [2.5 ... 3] [mm $°C^{-1}$ d^{-1}]
3. Cluster: High Mean Elevation and Slope, Low Latitude -> rather high DDF, range of [3 ... 3.5] [mm $°C^{-1}$ d^{-1}]

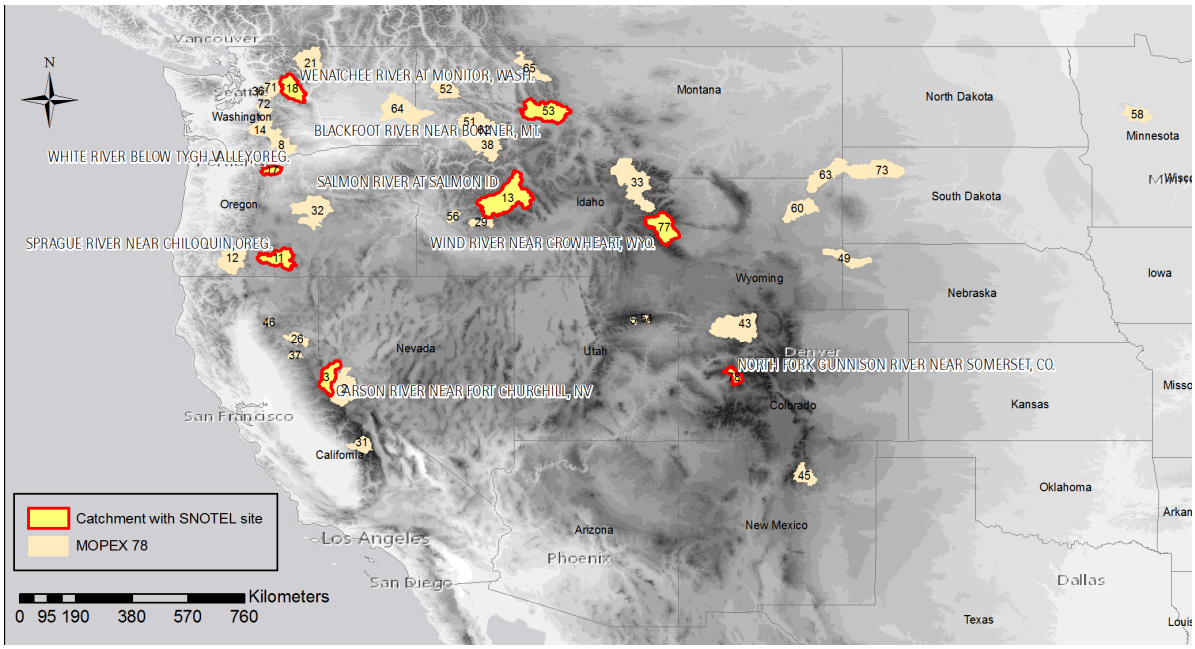

Figure 15: Catchments with SNOTEL sites: As SNOTEL SWE data is not available for every MOPEX catchment, we tried to find some matching ones as widespread and representative as possible. However, only the U.S.-west coast is currently covered by the SNOTEL project.

There would have been different approaches to classifiy the clusters, for instance by Berghuijs, Sivapalan, Woods and Savenije (2014), who used the aridity index, seasonality and timing of precipitation and fraction of precipitation falling as snow as their main arguments, but we determined to stick with simple topographic characteristics rather than with complicated vegetation-based approaches. Another step in this approach was to make DDF season-dependent, with a minimum in winter (50 % of maximum DDF) and maximum in Summer, realized via a linkage to EPOT (MATLAB script Main_Routine.m). An overview of MOPEX catchments and cluster types can be seen in fig. 16.

As described before, some literature values for model parameters from similar studies were taken, the remaining were calibrated. Schmucki et al. 2014 (p. 37) found “a high sensitivity to the TT distinguishing solid from liquid precipitation” in their study. For our study, comparisons with Berghuijs, Woods and Hrachowitz’s findings are intended , therefore the temperature threshold (TT) was chosen to be the same as in their study (1° C). Stahl et al. (2008) carried out a study in British Columbia, Canada: As the setting of this study was found to be similar to the MOPEX sites, the values for the fractional precipitation increase with height and the temperature lapse rate were adopted.

The Snowfall Correction Factor (SFCF) is of very high sensitivity regarding the model’s efficiency: it directly affects the input-parameter P as snow and, as a result, diminishes or increases the snowpack extent. As the mean areal precipitation data from the MOPEX dataset is based on computed values based on PRISM data (Daly et al. 1994), it was assumed that an extreme underestimation of snowfall would not be the case in our study. Therefore, the SFCF was only calibrated in a small range of 0

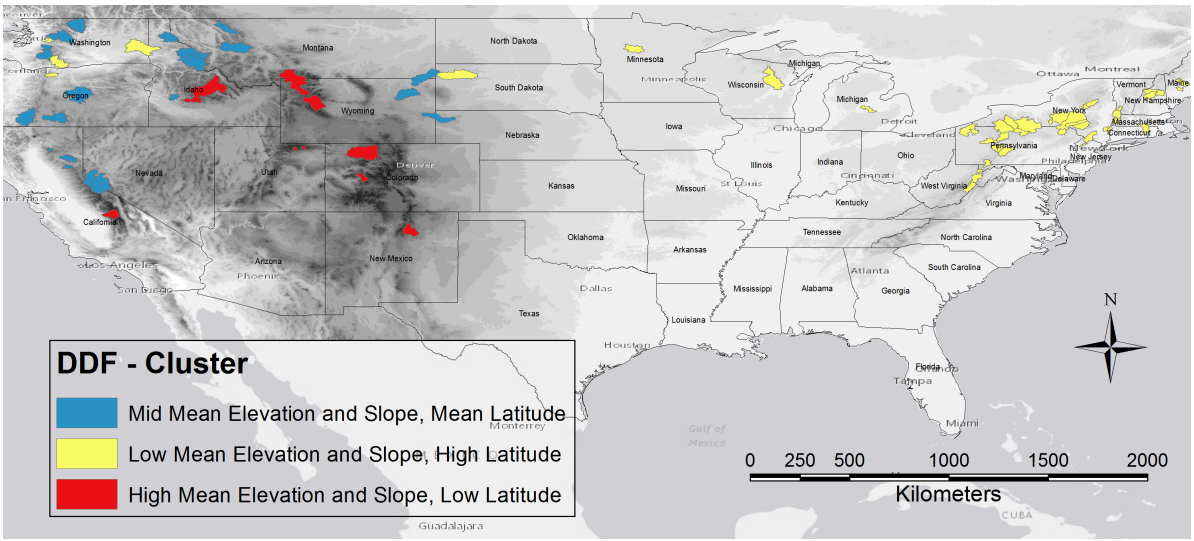

Figure 16: DDF-Cluster overview**:** An overview of the 78 snow-affected catchments and their distribution across the USA. The cluster colors mark the affiliation to one DDF-range, which will later be calibrated through the help of Monte-Carlo runs. The aspects over which the clusters were formed (by the help of a k-means approach) are slope, mean elevation and latitude.

to 20 %. CFR and CWH were both calibrated due to ranges recommended by Seibert (1997). When thinking about implementation of a rain-on-snow (ROS) factor , there was confidence of its importance due to several studies (Marks et al. 1998, McCabe et al. 2007, Freudiger et al. 2014). On the other hand, Valéry et al. (2014) had no improvement with the help of a ROS factor in their model. The decision was finally in favor of a ROS factor, as it can be implemented in the SAR easily and definitely has an impact on snowmelt rates during late winter. As ROS events are hard to quantify (Marks et al. 1998), it was chosen to be calibrated over a range of 0 to 0.2, which means that a ROS event can melt SWE up to 20 % of its volume. An overview of all parameters and their value or calibration-range can be seen in table 4.

2.3.2 Goodness of fit and Monte Carlo simulation

With 18 years of reference snow data for 8 catchments, we decided to use 9 years for calibration and 9 years for validation of our SAR. When thinking about which coefficient of determination should be used for evaluating the model's goodness, we first agreed on using the Mean Absolute Error (MAE) for comparing simulated SWE with SNOTEL references. For the MAE, we only took measured days with a snowpack and compared them with the simulated ones. This means that all simulated days with a snowpack are not covered by the MAE as long as there is no reference value on this day. Additionally, MAE has no information about total over- or underestimation, as it is unsigned. That's why the Mean Signed Difference (MSD) was chosen as a second coefficient of determination.

Another interesting factor in the goodness of a SAR is the total difference of measured to simulated snowpack days (DMS). A good impression of the preciseness of beginning and end of our simulated snowpack is of high value for this thesis. Additionally the MAE was set in relation to the maximum snowpack per catchment to provide better comparability between the catchments. An important measure of the model performance is the Nash-Sutcliffe-Efficiency (NSE) , also called efficiency

Table 3: Overview of coefficients of determination and their formula

coefficients of determination	formula	factors
Mean absolute error (MAE)	$\frac{1}{n}\sum_{i=1}^{n} \mid e_i \mid$	$\mid e \mid$= modulus of error
Mean signed difference (MSD)	$\sum_{i=1}^{n} s_i - r_i$	s = simulated value; r = reference value;
MAE to max. snowpack	$\frac{\frac{1}{n}\sum_{i=1}^{n} \lvert e_i \rvert}{snowpack_{max}}$	$snowpack_{max}$ = maximum of simulated snowpack
Difference of measured to simulated days (DMS)	$SD_{ref} - SD_{sim}$	SD_{sim} = simulated sum of days with snowpack $>$ 0; SD_{ref} = reference sum of days with snowpack $>$ 0
Nash-Sutcliffe-Efficiency (NSE)	$1 - \frac{\sum_{i=1}^{n} \left(r^i - s^i\right)^2}{\sum_{i=1}^{n} \left(r^i - \overline{r}\right)^2}$	s = simulated value; r = reference value;

criterion (J.E. Nash and J.V. Sutcliffe 1970). The NSE refers to the whole hydro-year, whereas the other presented coefficients only refer to measured days with snowpack $>$ 0, which was the reason for calibrating the SAR based on NSE. An overview of all coefficients of determination an their formula can be seen in table 3.

After having established all parameters, their calibration ranges and the coefficients of determination, we ran 25000 Monte Carlo runs: For each run, calibration parameters were based on random values within the calibration range, simulating 9 years of snowpack for the 8 SNOTEL-related catchments. NSE was calculated according to the SNOTEL reference values. As SNOTEL station's elevations were known, a short routine was implemented to compare a simulated SWE of the same elevation by taking the weighted mean of the two height zones below and above the SNOTEL station (see fig. 17). With the Monte Carlo runs completed, the best parameter set was taken in the end, respectively the maximum sum of all NSEs in a single run . For control purposes, plots were generated (MATLAB script Main_Routine_Val_Test.m). An example is shown in fig. 17.

It was also tried to use MAE or a mix of MAE and NSE for the validation of the models efficiency, but finally NSE was most convincing to produce the best results. Still, all coefficients of determination are meaningful when talking about the model's efficiency as can be seen in table 5. In table 4, a summary of all model parameters and their final values is shown.

2.3.3 Validation

For the model's validation, the last 9 available SNOTEL years were taken, respectively 1993 till 2001. The results of the validation period derived from the formerly calibrated values can be seen in Table 5 on page 37. MAE and MSD values show high correlation, showing that the snowmodel either under- or overestimates the current snowpack in most cases. The table also shows that the relationship of MAE to maximum snowpack of a hydroyear lies around 0.2, which means the models error typically lies around 20 % of the maximum snowpack extent. A similar study about a distributed snow model in southwestern Idaho found a MAE of 104 mm or 40 % of the mean basin SWE (Winstral et al.

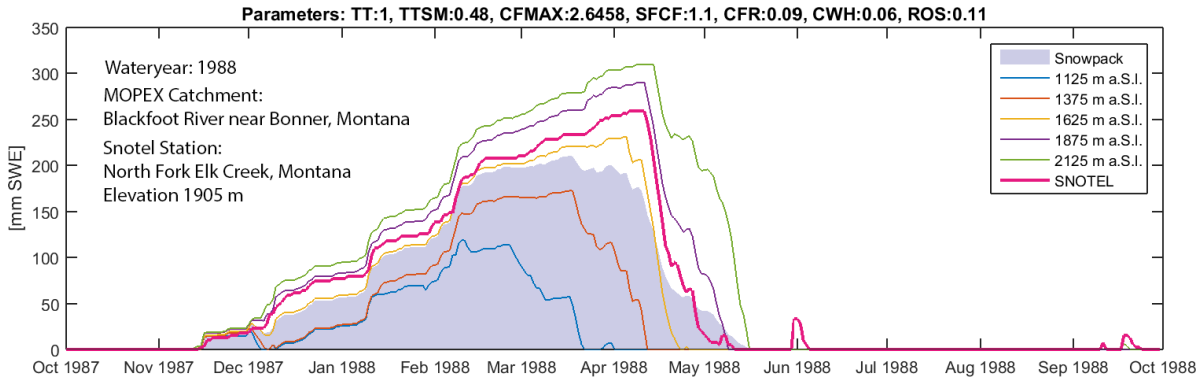

Figure 17: Calibration of Parameters: Control plot: The gray area depicts the SWE of the simulated snowpack. The thin colored lines are the catchments mean height zones in a 250 m - stepping. The thick pink line shows the SNOTEL stations measured SWE values. The station height of the SNOTEL station is 1905 m, which means the purple height zone should ideally be closest to the pink line, which is not exactly the case here. In general, this water-year seams to be simulated with high efficiency.

Table 4: Overview of literature and calibrated model parameters

		Literature	
Parameter	**Description**	**Value**	**Citation**
PGRADH	Fractional precipitation increase with height [mm/m]	0.0001	Stahl et al. (2008)
TLAPSE	Temperature lapse rate [°C/m]	0.0056	Stahl et al. (2008)
TTSF	Temperature Threshold Snowfall [°C]	1	Berghuijs, Woods and Hrachowitz (2014b)
		Calibrated	
Parameter	**Description**	**Value**	**Monte Carlo Range**
SFCF	Snowfall Correction Factor [-]	1	1 - 1.2
CFR	Refreezing Coefficient [-]	0.09	0 - 0.1 (Seibert 2010)
CWH	Water Holding Capacity [-]	0.05	0 - 0.2 (Seibert 2010)
TTSM	Temperature Threshold Snowmelt [°C]	1.29	0.4- 2
ROS	Rain on Snow Factor [-]	0.09	0 - 0.2
CFMAX	Degree Day Factor [mm $°C^{-1}$ d^{-1}]	[2.25 2.53 3.40]	[1.5-2.5]; [2.5-3.5]; [3.5-4.5];

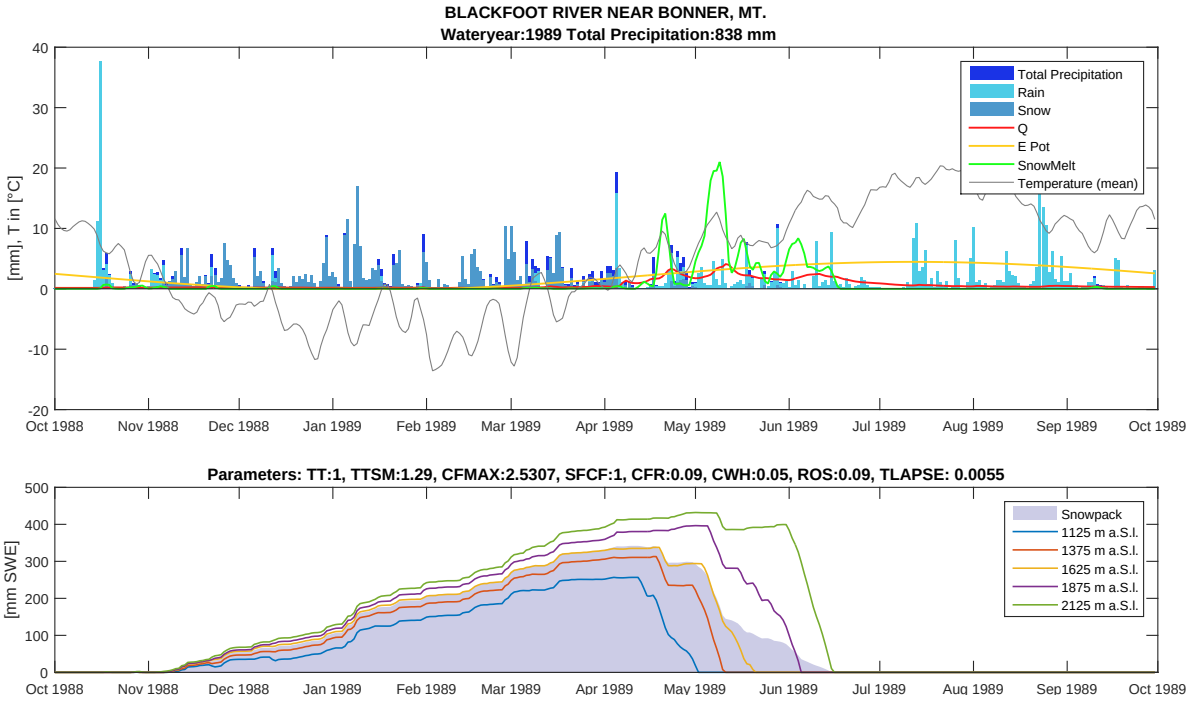

Figure 18: Example control plot of the snow models functionality: The upper subplot shows precipitation rates and forms. We also see the streamflow as red and the potential evaporation as yellow line. The green line depicts the 5-day floating average of the snowmelt rate. The catchment is situated in Colorado, with generally low precipitation rates especially during summer. Therefore, rising streamflow during April/May can be referred to snowmelt. Clearly, large amounts of snowmelt in this catchment are lost to evaporation, as we can see from the yellow line marking the progress of annual potential evaporation. The bottom subplot shows SWE alterations of the snowpack. Blackfoot River catchment is part of DDF-Cluster 2, as can be seen from the CFMAX-value.

2014). A study by Schmucki et al. (2014) in the Swiss alps had MAEs ranging between 161.4 mm (uncalibrated) and 43.8 mm (calibrated) of SWE.

Unfortunately, only western U.S. states are part of the SNOTEL program, so there's no reliable information about the northeastern MOPEX catchments. Besides, regarding the goodness of the snow model, the SNOTEL dataset itself is not guaranteed to be totally exact. On the one hand, several studies show the uncertainty of snow measurement devices (Yang 2014). On the other hand, regarding the measurements themselves to be correct, still differences in early seasons snowfall extent results in an offset concerning the whole season and therefore strongly affect the MAE. The DMS values show that the modeled snowpack exceeds the measured snowpack in all cases.

One important aspect in the visual control of simulated data is to check if the snowpack is being melted entirely over the summer period. If part of the snowpack would be transferred from year to year, there is a slight possibility of establishing a gigantic snowpack, as its CWH would get larger until no snow would melt at all. The MATLAB snowroutine has a built-in approach to set such years to "NaN".

Another point in visual control is to get an idea about the interaction of snowmelt and streamflow, like it is depicted in fig. 18.

Table 5: Overview of SNOTEL Sites and coefficients of determination for calibration (1984 till 1992) and validation (1993 till 2001) period:

SNOTEL Site	Height [m]	Mopex Catchment	MAE [mm] SWE	MSD [mm] SWE	MAE rel. to Max Snowpack	DMS [d]	NSE
Fish Lake	1045	Wenatchee River at Monitor, Wash.	140.9 100.1	139.9 48.1	0.21 0.12	11 8	0.82 0.94
Taylor Butte	1533	Sprague River Near Chiloquin,Oreg.	32.4 32.9	28.5 20.4	0.38 0.2	13 15	0.66 0.83
Mc. Clure Pass	2885	North Fork Gunnison River, Co.	52.8 67.8	39.8 64.3	0.18 0.22	15 12	0.91 0.89
Poison Flat	2357	Carson River Near Fort Churchill, Nev.	67 79.9	34.4 25.3	0.59 0.48	13 18	0.71 0.84
Elk Creek	1905	Blackfoot River near Bonner, Mt.	38.4 64.5	-28.7 -60.3	0.16 0.19	15 25	0.86 0.74
Morgan Creek	2400	Salmon River at Salmon, Id.	35.8 28.4	18 14.5	0.19 0.12	14 19	0.92 0.96
Cold Springs	2935	Wind River near Crowheart, Wyo.	27.7 38.1	-3.5 -29.2	0.15 0.2	26 21	0.88 0.56
Clear Lake	1161	White River Below Tygh Valley, Oreg.	54.1 64.8	10 3.2	0.33 0.32	24 23	0.87 0.87
Total mean			**56.1** **59.6**	**29.8** **10.8**	**0.27** **0.23**	**16.4** **17.6**	**0.83** **0.83**

2.4 Statistical approach

Berghuijs, Sivapalan, Woods and Savenije (2014) used linear regressions to investigate inter-year variations in normalized annual streamflow (NAS, see equation 6) on a possible linkage to the fraction of precipitation as snowfall (SF). They found that a correlation between SF and P results in a spurious correlation between SF and NAS. To avoid that, they used a correction approach to calculate the P to SF correlation out of the SF to NAS correlation.

In order to avoid spurious correlations in our research, simulated data was tested on a possible correlation between total infiltration INF and P by the help of a linear-regression-approach. The results show a significant positive correlation between INF and P in all 78 catchments. In other words, a year with high precipitation rates causes high infiltration rates in all 78 catchments. The next step was to examine the probable link between NAS and P of a year. 60 of 78 catchments show a significant correlation, of which 4 with a negative and the remaining 56 with a positive slope. This means that in 56 catchments, high P is resulting in high Q and in the other 4 catchments the opposite is the case. The missing 18 catchments show no significant trend at all. The significance P-value limit was set up to 0.05 for model rejection as described in Grace et al. (2015). As a consequence of these tests, it is not possible to compare infiltration with streamflow without using a correction approach like Berghuijs, Sivapalan, Woods and Savenije (2014).

A common approach to deal with such cause-effect relationships in natural sciences is the one described by Grace et al. (2015): Structural equation modeling (SEM) helps to determine causal coincidences between input variables in a model and therefore avoids spurious correlations. In our case, we already tested the relation of P to NAS and P to INF for every catchment. According to Grace et al. (2015), the total effect E_{total} of INF on NAS can be computed as the sum of the direct and indirect pathways:

$$E_{total} = E_{direct} + E_{indirect} = E_{INF-NAS} + (E_{INF-NAS} * E_{P-INF}) \tag{3}$$

Another recommendation by Grace et al. (2015) is to use standardized effects in a study. Using the runoff coefficient (RC) for example standardizes the mean P-Q relation, which is common use in hydrology:

$$RC = \frac{\overline{Q}}{\overline{P}} \tag{4}$$

Via RC one can calculate the expected streamflow Q_{exp} per Year:

$$Q_{exp} = RC * P \tag{5}$$

Therefore, “Normalized annual streamflow” is:

$$NAS = Q_{measured} - Q_{exp} \tag{6}$$

The most positive side effect of using standardized effects is the comparability of different catchments, therefore Berghuijs, Sivapalan, Woods and Savenije (2014) applied it as well. The approach is also subject to criticism, thus it was not utilized for standardizing the infiltration ratio, as such “infiltration coefficient” is not commonly used.

A main goal of this thesis was to show that snowmelt makes the difference in streamflow due to higher infiltration rates compared to rain. Therefore the dimensionless ratio of snowmelt infiltration to rain infiltration (SIRI) can also serve as a comparison factor. This ratio has no correlation to precipitation in any catchment, as proven through linear regression tests. Thus, a SIRI ratio of 75 % just states that 75 % of a years total infiltration came from snowmelt, regardless of the precipitation amount. Additionally SIRI tells us that snowmelt was the main influencing factor for infiltration of that year, which also includes the relation to hydraulic conductivity in that specific catchment. To clarify, SIRI is described again:

Snowmelt infiltration to rain infiltration ratio (dimensionless):

$$SIRI = \frac{Snow_{Inf}}{Rain_{Inf}} \tag{7}$$

All MATLAB routines involved in generating the results can be overseen in tab. A.3 of the appendix.

3 Results

3.1 Simulated snowmelt rates

First, the snowmelt rates resulting from the modeling approach are presented. Fig. 19 shows the distribution of daily snowmelt rates of all catchments and years. The histogram illustrates that the data is Poisson-distributed, with the maximum of occurrences at a daily snowmelt rate near zero. The box-plot in fig. 19 points out that the median of the daily snowmelt rate is around 2 mm/d, with 50 % of all values ranging between 1 and 4 mm/d (all values inside the box). Including the 1.5-wise IQR (inter-quartile-range, a.k.a. whiskers), daily snowmelt covers the range of 0 to 8 mm/d. The outliers are starting from 8 and go up to 45 mm of molten SWE per day.

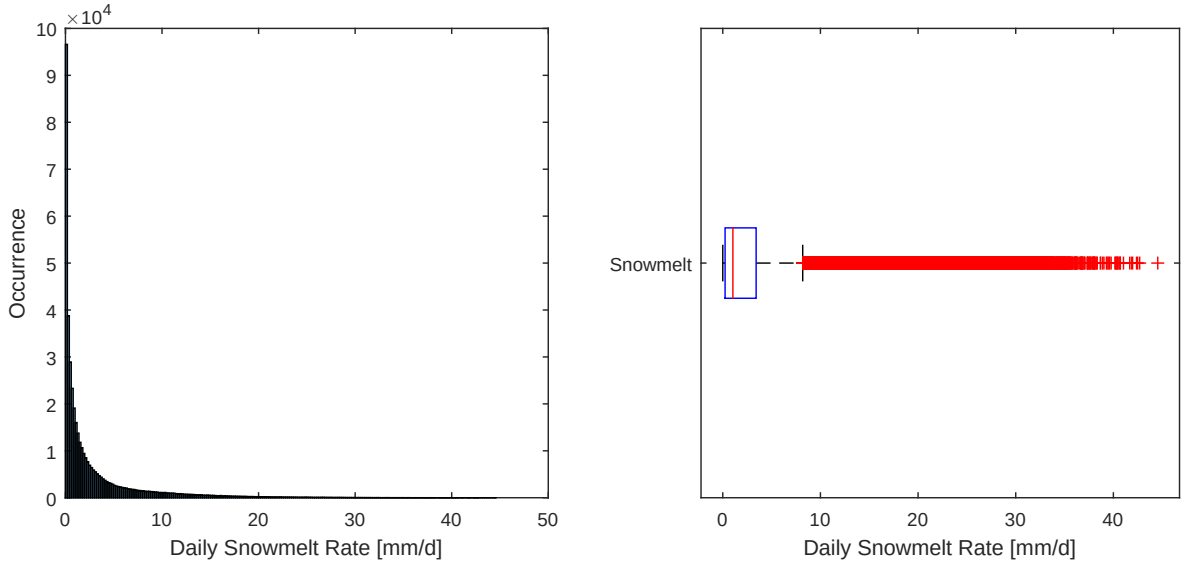

Figure 19: Overview of simulated snowmelt rates: A histogram (left) and a boxplot (right) show the (uneven) distribution of daily snowmelt rates for all 78 catchments and 53 years.

With the distribution of snowmelt data cleared, another question was if there were any regional patterns recognizable. An answer to this question can be seen via fig. 20: Regional patterns exist for most catchments, some with either high or low values for mean snowmelt rates and some just with high inter-year variability. Interestingly, the plot also points out temporal similarities, not to be totally explained at this point but probably being connected to warm/cold winters or differences in the intensity of the melting period. The predominant color of the plot is blue, stating that most common values for mean snowmelt rates are between 1 and 4 mm/d.

The next step was to compare simulated snowmelt rates with hydraulic conductivities, to get a clue if they depict a barrier for the percolating water, as being assumed in the hypothesis of this work. In fig. 21, we learn that the relation between K and snowmelt rates is of very high variability: Approximately a quarter of all catchments has high hydraulic conductivities (more than 8 mm/d), depicting no barrier for mean daily snowmelt rates. This does not imply that no snowmelt is ever blocked by the conductivity, as we are dealing with mean snowmelt rates here. In contrast, very low hydraulic conductivities $<$ 1mm/d are the case in another quarter of all catchments. Again, due to the fact that the plot shows mean snowmelt rates, infiltration is still possible. Half of all catchments have their conductivity inside or very close to the range of snowmelt rates. These catchments are

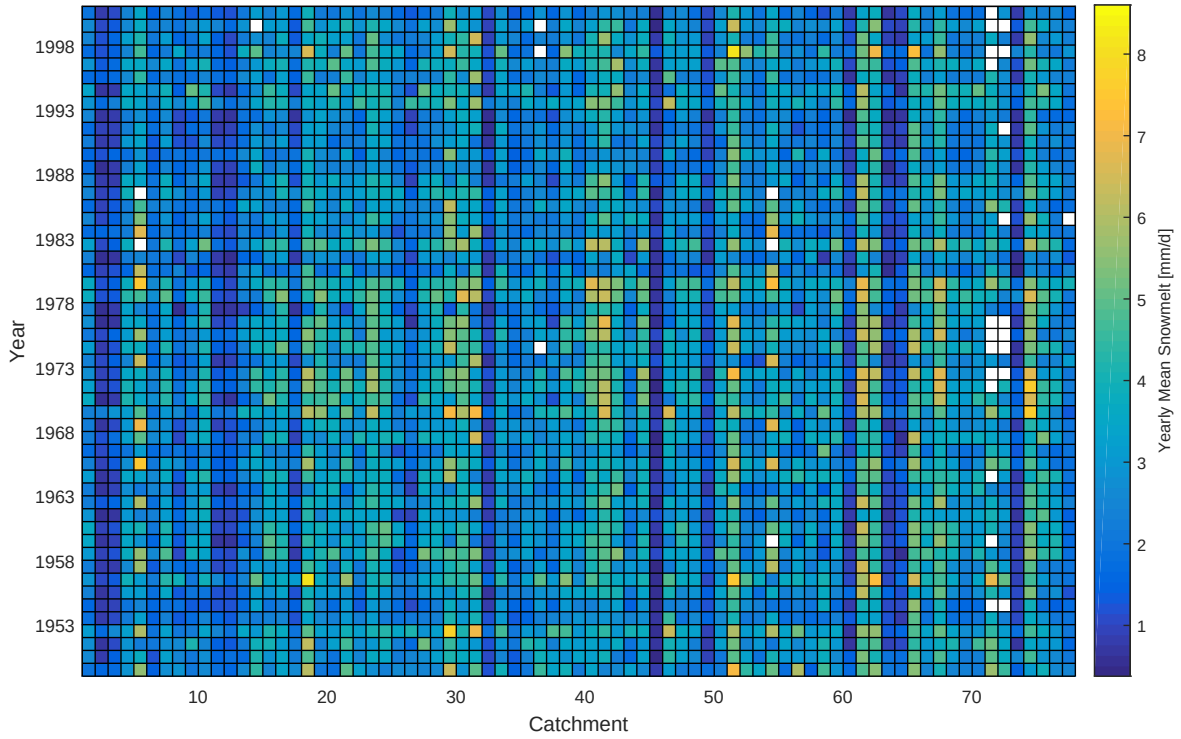

Figure 20: Pseudocolor plot of yearly mean snowmelt rates per Catchment: One can see a regional and temporal display of yearly mean snowmelt rates. White boxes demonstrate missing data. Variation between catchments is clearly visible, but even temporal similarities can be recognized. The catchments are not sorted to a specific order.

of particular interest in terms of comparing snowmelt rates to rain intensities, as they might let pass the majority of snowmelt but state a barrier for rain events. A major interim result hereby is, that many catchments probably have to be excluded from our hypothesis, as they don't represent a barrier at all. On the contrary, some conductivities are so low, that they won't pass snowmelt or rain regardless of its intensity.

When looking at precipitation and snowmelt intensities, the comparison plot of mean daily snowmelt-, rainfall- and snowfall-rates shown in fig. 22 provides further insights: As expected, simulated daily snowmelt rates are lower than daily rain rates. The difference is smaller than expected and ranges between 0.25 mm and 1 mm, making it's impact on the catchment's water balance questionable. To make a statement on the percentage of snowmelt which is actually "blocked" by K in a catchment, one has to look at fig. 23, showing the result of calculating a yearly ratio of "blocked snowmelt" to total snowmelt. Similar to fig. 21, high variability between catchments can be observed: Some catchments are of permanently high (more than 90 %) or very low (less than 10 %) "blocked"-ratios. The field in between is marked by some catchments with a small range in inter-year variability as well as by catchments which almost range over 50 % of the scale. Another result given by the plot is that the yearly "percentage of snowmelt blocked by conductivity" is mostly normal distributed (centered median lines inside the boxes). This also means that the whiskers of the boxes cover 95 % of all data. Outliers are the exception, only meteorological extreme years produce extraordinary high or low "blocked" ratios in a catchment. Aside from that, the comparison of fig. 23 with fig. 21 points out that most catchments are actually influenced by low hydraulic

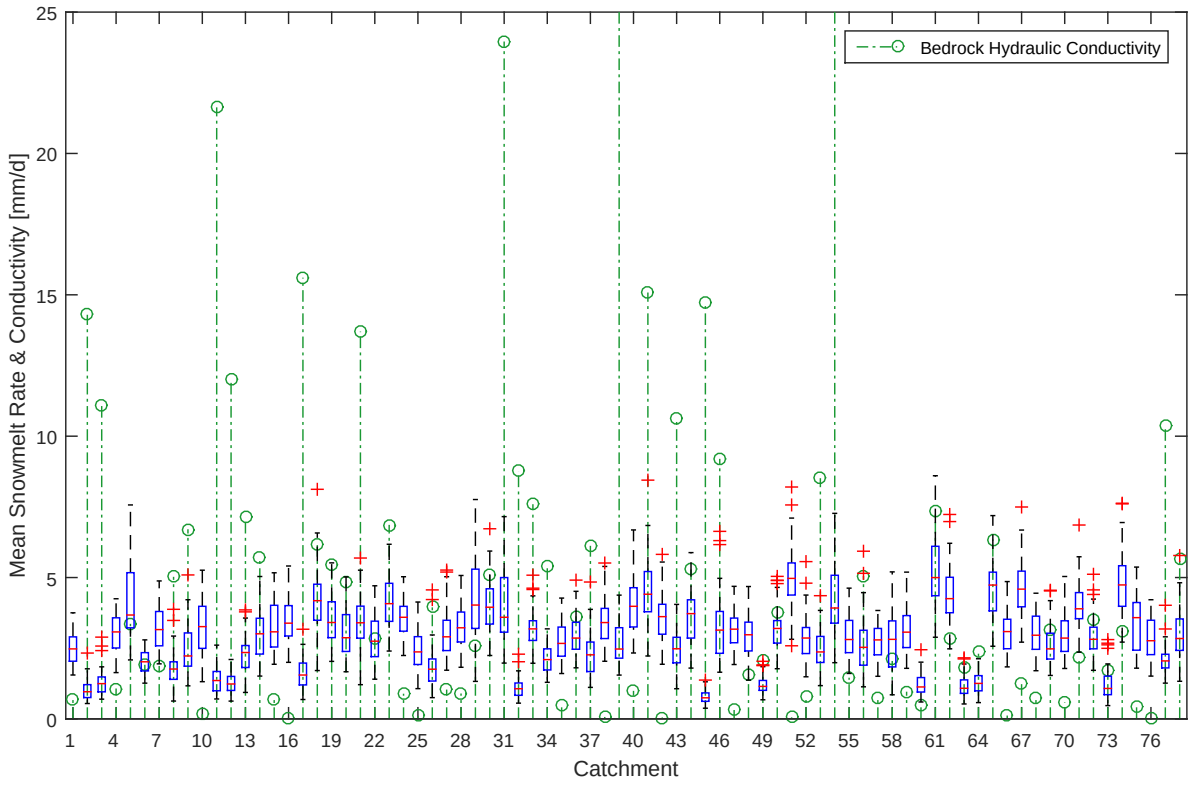

Figure 21: Box-plot overview of mean hydraulic conductivities and snowmelt rates on catchment scale: The plot includes one boxplot per catchment, showing the catchment's distribution of mean snowmelt rates. Additionally there's a green dot which demonstrates the mean hydraulic conductivity of the catchment and a dashed line up to the point, emphasizing its position. The plot's y-axis limit has been shortened to be able to see details of the box-plots, hence few very high conductivities have been cut off.

conductivities. Having learned about ratios of snowmelt being blocked by K, the next question to answer is if there is a difference between blocked snowmelt- and rain ratios. Fig. 24 shows that both blocked snowmelt and rain ratios range from 0 to 100 % but the median of snowmelt rates is 15 % lower.

3.2 Comparison of infiltration into bedrock for snowmelt and rain

The main hypothesis includes that infiltration into the bedrock is essential for the main streamflow of the catchment. Therefore, this section concentrates on the question, what actually causes the difference between more rain or snow infiltration into a catchment's bedrock. Ratios of yearly "blocked" snowmelt and rain were already presented. Now, the focus lies on "snowmelt infiltrated ratio" (SIR) and "rain infiltrated ratio" (RIR), both to be understood relative to total snowmelt or rain of a year. A SIR of 0.4 for example means, that 40 % of a years total snowmelt can directly percolate into the bedrock, contributing to the groundwater. A RIR of 0.8 thus means, that 80 % of a years rainfall contributes to the groundwater of the catchment.

The difference of SIR - RIR combines both quantities. Negative values represent higher percentual rain infiltration, whereas positive values stand for higher snowmelt infiltration of a catchment. This difference gives no information about the importance of snowmelt to the catchments total infil-

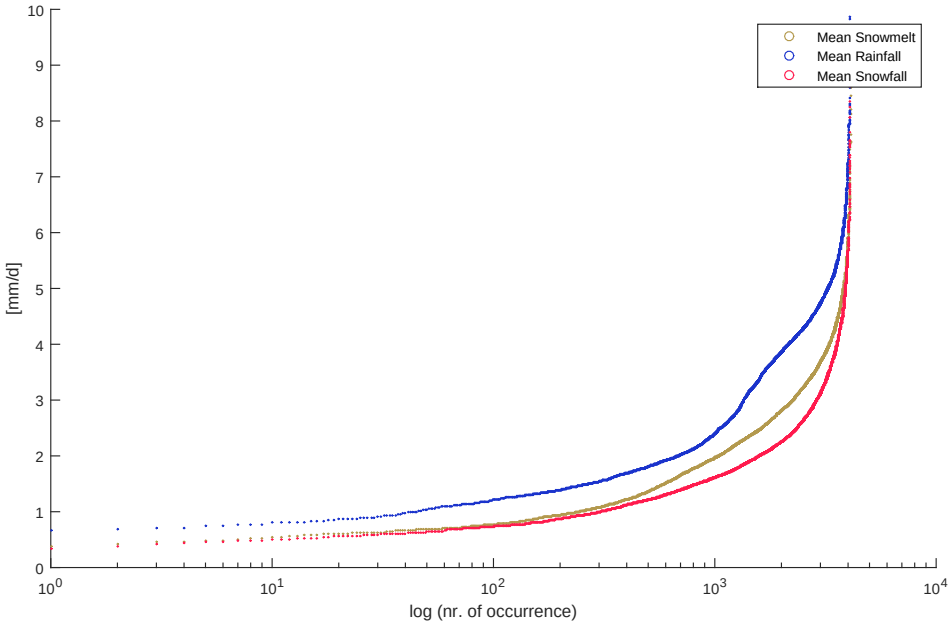

Figure 22: Comparison of mean snowmelt to rainfall and snowfall: Depicted are ascending sorted mean snowmelt-, rain- and snowfall rates of all catchments. The x-axis is shown logarithmic and the y-axis has been limited for better clarity.

tration, but we can learn about patterns which dominate a catchment's infiltration contribution. Fig. 25 shows what was being expected: in most catchments SIR is higher than RIR, which can be ascribed to lower snow infiltration rates in average. And yet there are some catchments with constantly higher RIR: To find an explanation for this, a map with mean SIR-RIR differences was created (fig. 26), to see if there are any regional patterns noticeable. Additionally, the two most extreme catchments were picked (high SIR: catchment 37 in fig. 27 and high RIR: catchment 33 in fig. 28) and closer examined on their seasonal snowmelt and rain behavior. When studying the map in fig. 26, most catchments with high RIR are found across the Rocky Mountains.

The highest RIR is the one by Yellowstone River catchment near Livingston in Montana, draining from the Rocky Mountains. High SIR rates are found to be either in very continental zones or in mild climates near the coast. The highest SIR is found in the North Yuba River catchment below Goodyears Bar in California, a catchment draining from the Sierra Nevada. To understand the difference between those two catchments, a closer look on the simulated snowmelt rates of those catchments must be taken: Fig. 27 shows wateryear 1980, a year found to be representative for the catchment's basic snowmelt regime. The plot underlines that year's extreme climate, with extremely high winter precipitation rates and a distinctive dry summer season. Furthermore, it is a catchment with a wide variety of elevation zones, ranging from 1100 up to 2400 m. The mean temperature curve shows a mild winter, but warm summer. Due to the temperature-height gradient used in our model, we have a large variety of snowpack SWE. The lower elevation zones in this catchment are almost snow-free, whereas the three upper elevation bands can maintain their snowpack from January till April. From May till July the snowpack melts completely, contributing strongly to runoff rates during summer. Due to the lack of regular rain events during summer in this catchment, runoff must mainly be fed by snowmelt.

The fact, that this effect can be seen through simulated data, is a good example for the proper

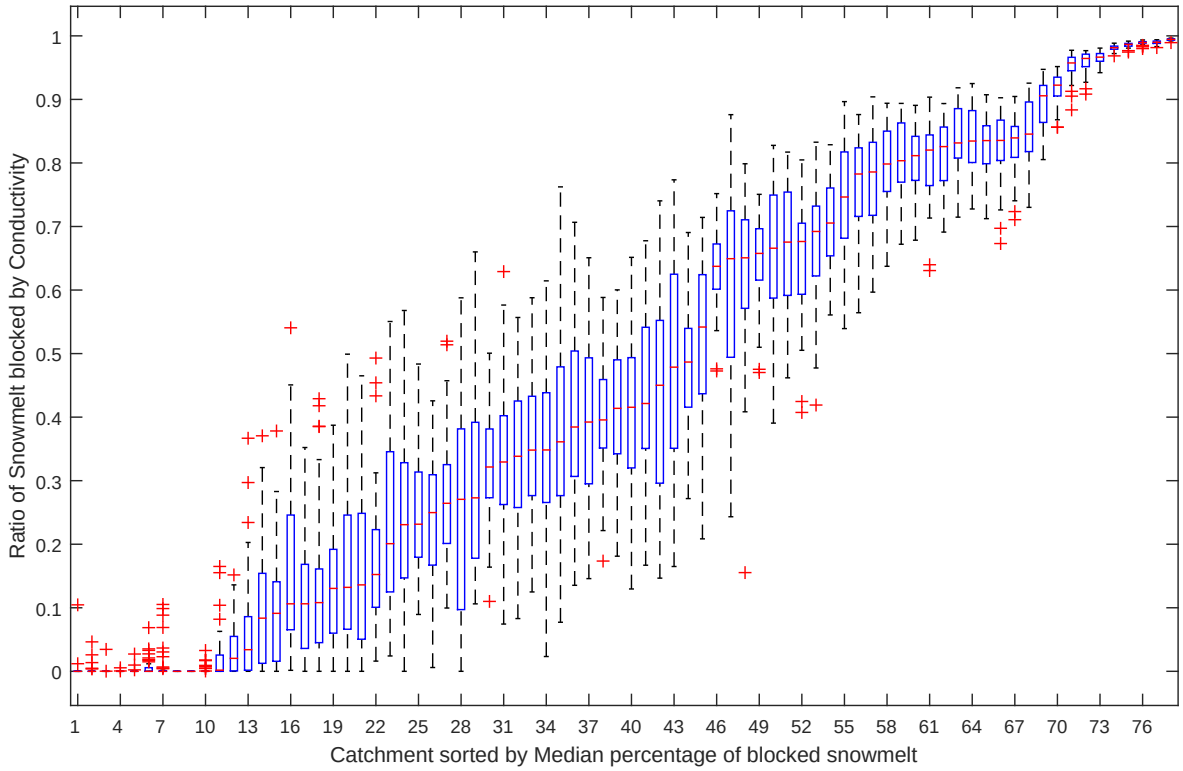

Figure 23: Box-plot overview of snowmelt ratios being "blocked" by hydraulic conductivity per catchment: The catchments have been sorted ascending by their median value. The input data of this plot depicts the difference of snowmelt rates on a daily basis and the hydraulic conductivity of the catchment. A yearly sum of total "blocked" snowmelt is calculated and set in relation to the years total snowmelt. Done for all 53 years, the box-plot shows the range of "blocked" ratios of snowmelt for all 78 catchments. Some catchments with a constant zero percent of blockage are hardly visible, they are only depicted by a single horizontal red line at the very bottom of the plot.

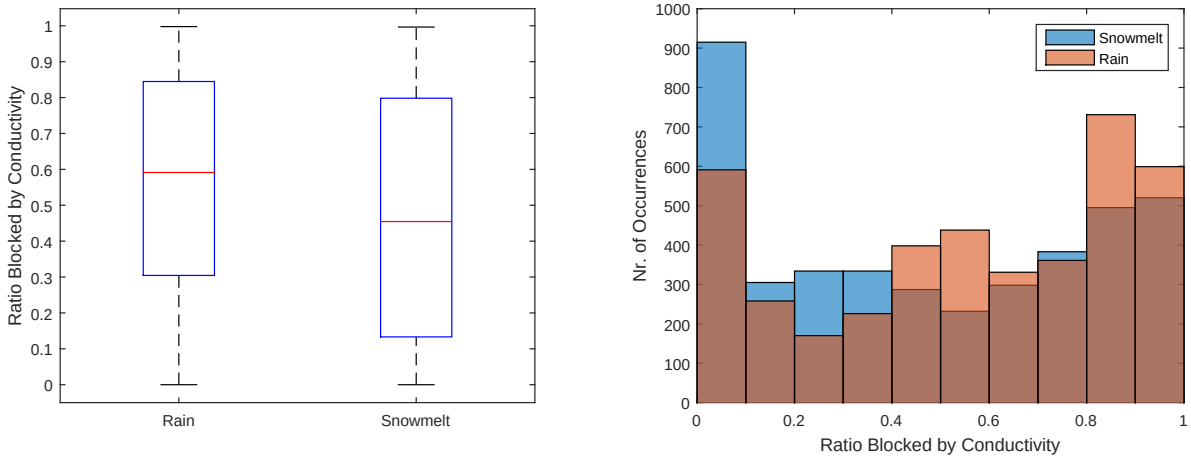

Figure 24: Combined plot comparing "blocked" rain and snowmelt ratios: The box-plot on the left shows the distribution of "blocked" ratios of rain and snowmelt for all catchments. The histogram on the right underlines the fact that ratios of blocked snowmelt are smaller than ratios of blocked rain.

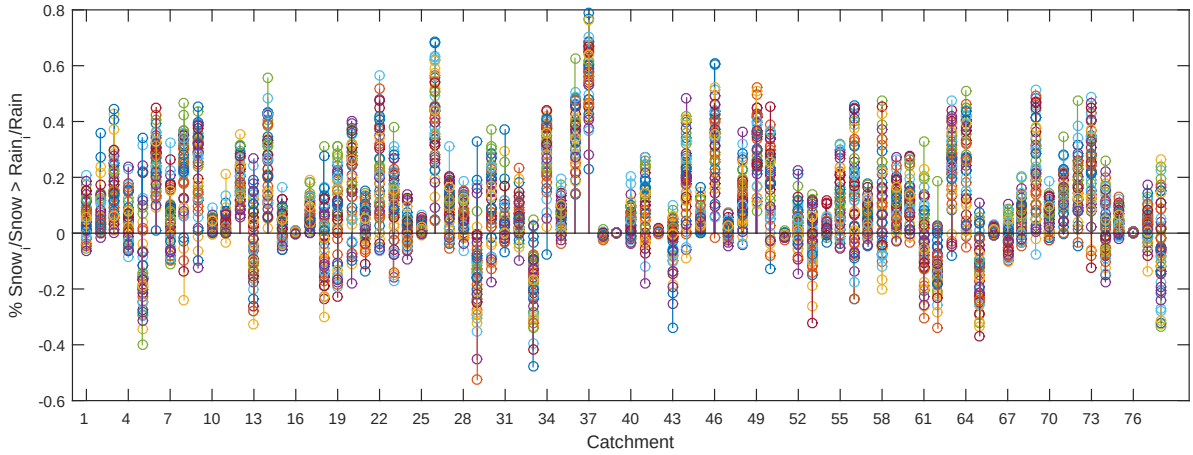

Figure 25: Stem plot of "snowmelt infiltrated ratio" (SIR)minus "rain infiltrated ratio" (RIR): Stems below the zero-axis represent a wateryear of a catchments with higher rain infiltration than snow infiltration on a percentage basis. Stems above the zero-axis represent higher snowmelt infiltration rates.

functionality of the snow model. The long snowmelt period is also the answer to extremely high SIR compared to RIR in this catchment: The snowmelt period is effectively lasting over 6 to 7 months, whereas rain events are seldom and intense. A completely different view can be seen in fig. 28. Wateryear 1980 of Yellowstone River catchment shows a total precipitation of 775 mm with a focus on rain during winter till early summer. The catchment's elevation bands show that its mean elevation is about 500 m higher than the Yuba River catchment, but with the same number of elevation bands. Most remarkably, the temperature range during wateryear is more distinct, with a cold winter and a warm summer. This factor leads to a very short melting period, in which the catchment's snowpack loses 200 mm of SWE in one month and the remaining 100 mm in another. On closer inspection, rising discharge rates in late April and mid May can be seen, without any rainfall during these episodes: The snow model demonstrates again it's efficiency, as snowmelt is obviously the only contributing factor here.

Yet, there's no explanation to the exact processes underlying, as evapotranspiration rates as well as groundwater recharge would have to be taken into consideration. But still these two catchments give a good impression of the applicability of the built snowmelt routine and the two most diverging snowmelt behaviours: A long melting period with constantly low snowmelt rates (due to rather mild, maritime climate), and a short and intense phase of snowmelt (distinctly warm summer and cold winter, continental climate). Hereby, it must also be mentioned that hydraulic conductivities of the two presented catchments were similar (between 6 and 7 mm/d). Getting back to fig. 25 there are few catchments that don't vary between SIR and RIR. Those were found to be the catchments with extremely low hydraulic conductivities ($<$ 1mm/d).

3.3 Connectivity between infiltration rates and streamflow

Final regression analyses between INF and NAS show 43 significant correlations. For SIRI and NAS there are 33 significant correlations. The result is visualized in fig. 29. The most significant trend hereby is that high infiltration rates induce high streamflow in many catchments. However,

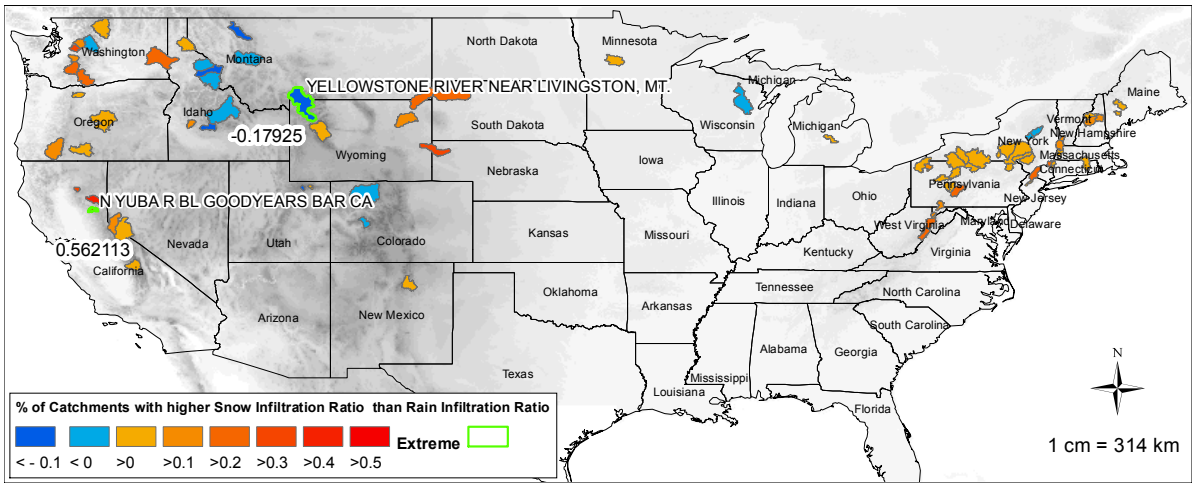

Figure 26: Overview map of mean snow infiltration ratio to rain infiltration ratio: The colorbar shows negative values for SIR-RIR blueish, and positive values in orange to red. Both the lowest and the highest catchments are extra pointed out green. Their SIR-RIR value is additionally labeled to the catchments name.

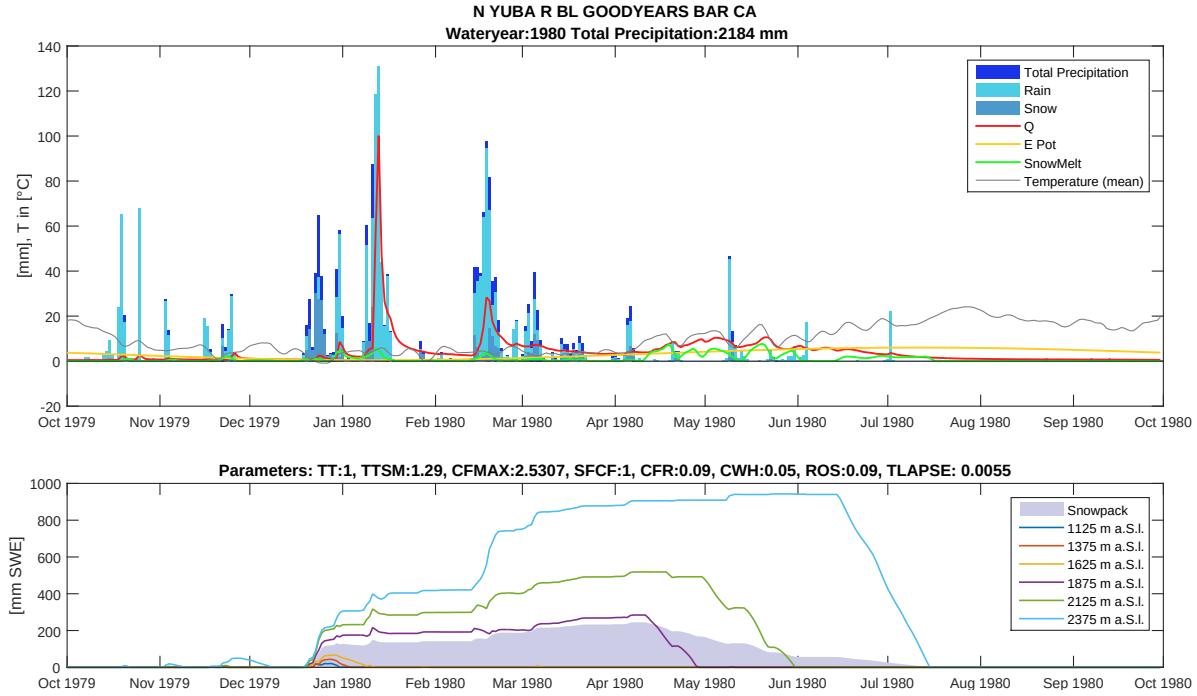

Figure 27: Wateryear 1980 of North Yuba River catchment (high SIR): The bottom subplot shows the snowpack to be completely relying on the 3 upper elevation bands, melting from April to July and influencing the catchments streamflow during summer (upper subplot).

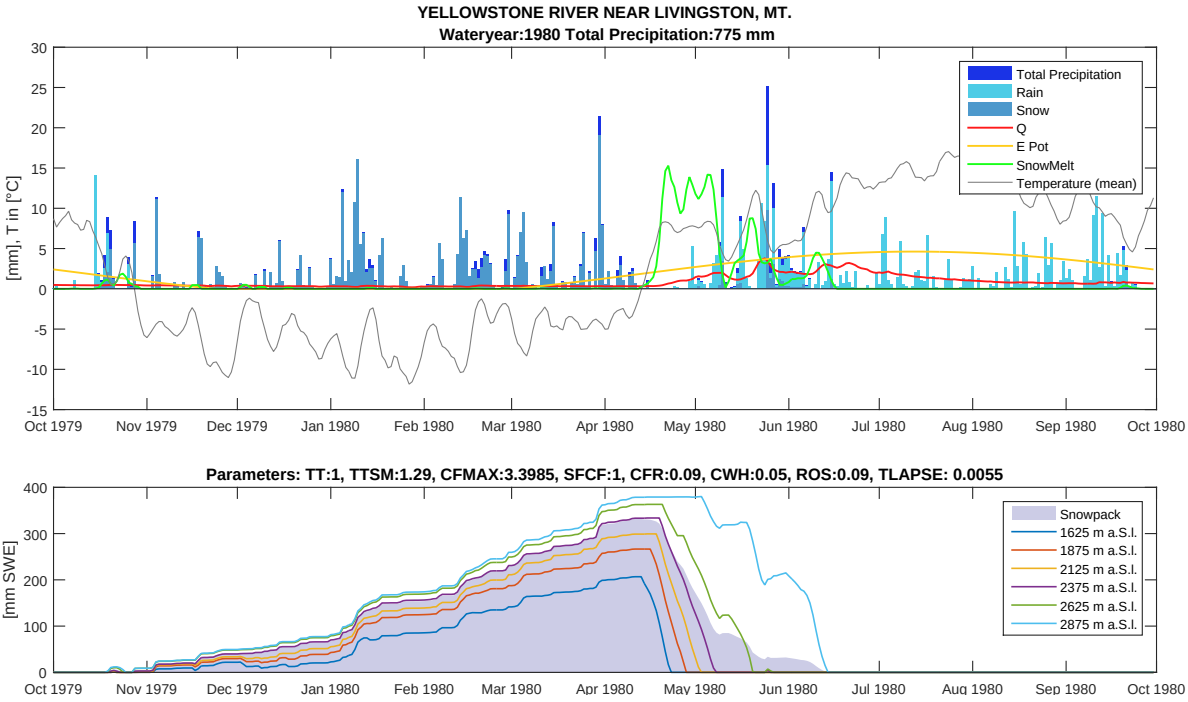

Figure 28: Wateryear 1980 of Yellowstone River catchment (high RIR): The snowmelt period can be characterized as “short and intense”. All elevation bands are involved, lowering the snowpack SWE down by 200 mm in less than a month.

3 catchments do not follow that trend, stating that more surface runoff would result in higher streamflow. The catchments with a positive INF-NAS trend seem to be more dense at the U.S. west coast and the northeast. Continental catchments seem to be less affected by this trend.

Regarding the positive SIRI-NAS-effect (17 catchments), there is numerous overlapping with the INF-NAS effect. With a higher percentage of snowmelt infiltrating than rain, higher streamflow is induced. Those are the very catchments, which confirm our hypothesis. There is a single catchment with a negative SIRI-NAS correlation. Interestingly enough, it has still got a positive INF-NAS correlation, which will be discussed later on.

In fig. 30, the sensitivity of NAS against INF is depicted. The column between 0.2 and 0.4 on the x-axis shows that 20 catchments result in a 20 % to 40 % increase in NAS, whan infiltration capacity is twice the normal infiltration capacity. The most left column indicates that there is one catchment with up to 60 % less streamflow at twice the infiltration capacity. This illustrates the influence of infiltration capacities on annual streamflow in 50 % of our catchments. SIRI supports this pattern, but only for less than the half of all catchments (see fig. 31): A 25 % increase in the annual SIRI is able to increase streamflow between 25 % to 50 % in 13 of our catchments, to describe one of the columns. Therefore, the results are partly able to support the study by Berghuijs, Sivapalan, Woods and Savenije (2014), but show no general pattern between snowmelt, conductivity and streamflow for all 78 catchments.

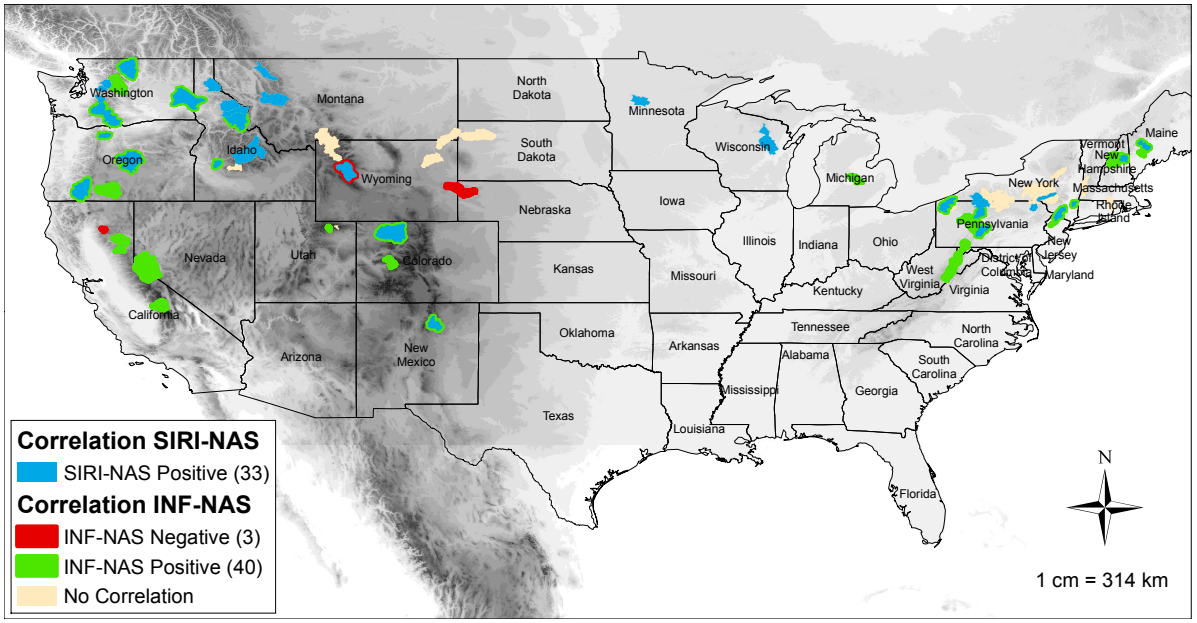

Figure 29: Occurrence and connectivity between infiltration- streamflow effects: The map shows significant correlations between INF and NAS as well as SIRI and NAS. In catchments with both effects, the outline color of the border line represents the hidden correlation. The beige colored catchments show no significant correlation at all. There is no information about the intensity of the effects given here. The map is intended to show just the positive/negative trend.

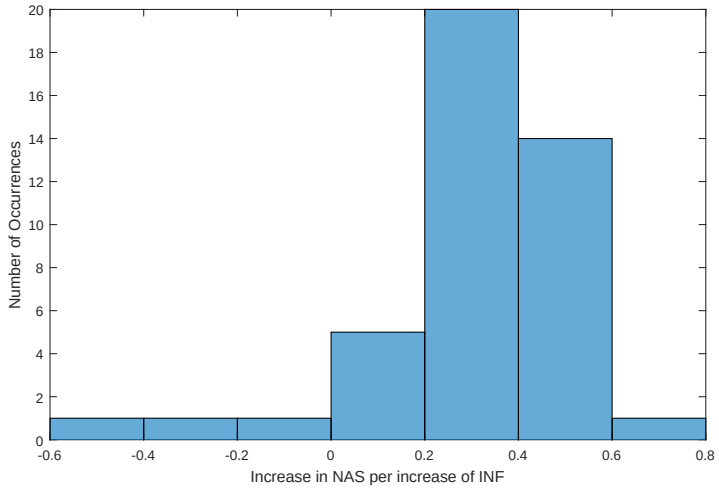

Figure 30: Sensitivity of normalized annual streamflow to normalized infiltration: The histogram depicts the change in normalized annual streamflow (NAS) per unit change in the annual normalized infiltration (INF) for 43 catchments with a correlation between INF and NAS.

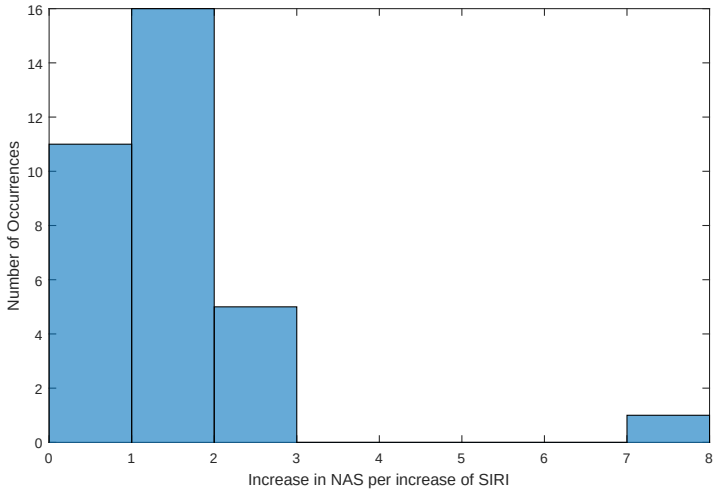

Figure 31: Sensitivity of normalized annual streamflow to composition of infiltration: The histogram shows the change in normalized annual streamflow (NAS) per unit change in the annual normalized infiltrated snowmelt/rain ratio (SIRI) for 33 catchments.

4 Discussion

The results demonstrate, that average simulated snowmelt rates are below rain rates, as expected and proposed in the hypothesis. Mean snowmelt rates vary between catchments and show regional and temporal patterns. It was possible to show that hydraulic conductivities in the 78 catchments are usually at the same scale as snowmelt and rain rates, between 2 and 10 mm/d. Up to this point, there was high confidence in the thesis of "bedrock as a barrier" for infiltrating water, as it could also be shown that snowmelt rates were more likely to infiltrate into bedrock. Yet some catchments have to be excluded up to this point by showing either too low or too high hydraulic conductivities.

In the next step, it was demonstrated that in some catchments snowmelt infiltration dominates rain infiltration. A possible explanation for this finding was given through the closer examination of two catchment's melting periods, one short and intense, the other lasting over half a year with constant low snowmelt rates.

Finally, statistical analysis brought up correlations between infiltration rates and streamflow as well as the composition of the infiltrated water (rain/snowmelt) and streamflow. Yet, this finding only applies on 50 % of the catchments. So what about the outcomes of this study? How good are the "partial" results and is there a point in still maintaining the initial hypothesis? Which assumptions were maybe too optimistic? Which factors were ignored by our approach? Is it possible to finally make a general statement about climate change and linked changes in snowmelt and streamflow behavior? Those questions are to be answered in the following.

4.1 Influences of the simplified main approach on the studies results

Some general simplifications of hydrological processes were made upon the realization of this thesis, of which the most influencing are:

- Assumption of permanently saturated soil-water conditions
- Assumption that only bedrock represents a barrier for infiltrating water, soils were being

ignored

- Frozen soils could represent a strong barrier for infiltrating water, a factor that is totally ignored
- Vegetation and land use are not being considered at all

Mean hydraulic conductivities of the MOPEX catchments in this study were found to be ranging between 2 and 10 mm/d, as demonstrated in fig. 10 and fig. 11. When using the geometric mean for calculating conductivity on catchment scale by referring to Gleeson et al. (2014), proper transformation of the standard deviations of the original data was of high priority: By applying the Gauss'ian uncertainty propagation calculation on the original standard deviations of the global permeability map, it was further possible to show standard deviations for the mean hydraulic conductivity of each catchment. Standard deviations are varying between catchments, most of them in the magnitude of 1/4 to 1/3 of the actual conductivity, values which are pretty high regarding snowmelt and rain infiltration. When comparing these values with Gleeson et al. (2014), its understood that the problem already comes from the original data, as the geological categories for bedrock are based on wide ranges. In terms of the results of our thesis this means that infiltration rates will be over/underestimated up to 25 % of the actual values, as following example can show:

A catchment with a K of 6 mm/d and a standard deviation of 2 mm/d could also be represented by a K value of 2 respectively 4 mm/d (-2 or -1 standard deviations). In the other direction, K-values of 8 respectively 10 mm/d would result from +1 or +2 standard deviations. These K values cover 95 % of all data, as long as they are normally distributed (Dormann 2013). Therefore, assuming 10 mm of potential infiltrating water on a single day, the infiltration range lies between 20 % up to 100 %. In conclusion to this, simulated infiltration rates must be considered to be vague. This also compromises the good correlation between infiltration and streamflow, as shown in chapter 3.3. Nevertheless, the relation between snowmelt and rain infiltration should only be weakly affected by this uncertainty, as snowmelt rates were shown to be generally lower than rain rates for most catchments.

Seyfried et al. 2009 (p. 858) state that "streamflow initiation and cessation are closely linked to the overall watershed soil water storage capacity, which acts as a threshold." In a modeling approach, they found out that streamflow response would only be sensitive to snowmelt, if the soil water content was above this threshold. For current thesis, streamflow response time to snowmelt is not of particular interest, as only summed up streamflow amounts of the hydroyear were used. And similar to current study, for Seyfried et al. (2009) bedrock conductivity is still the limiting factor for the soil water content to reach its threshold. Migała et al. (2014) did research on soil moisture and temperature variation under different types of tundra vegetation. The found out that soil moisture during the growing season is mostly depending on the snow cover and the snowmelt rate. Soils show large fluctuations in their water content depending on their texture: Coarse texture provokes rapid infiltration into the lower parts of the soil profile. Furthermore, Migała et al. (2014) found out about the strong influence of thawing snow on soil temperature. It is induced by "increased solar radiation and air temperature, which increased the amount of ablation water flowing downslope" (p. 17). In case of the study by Migała et al. (2014), soils are seldom the limiting factor for snowmelt to infiltrate, therefore our assumption of bedrock as the "limitation" regarding infiltration could be

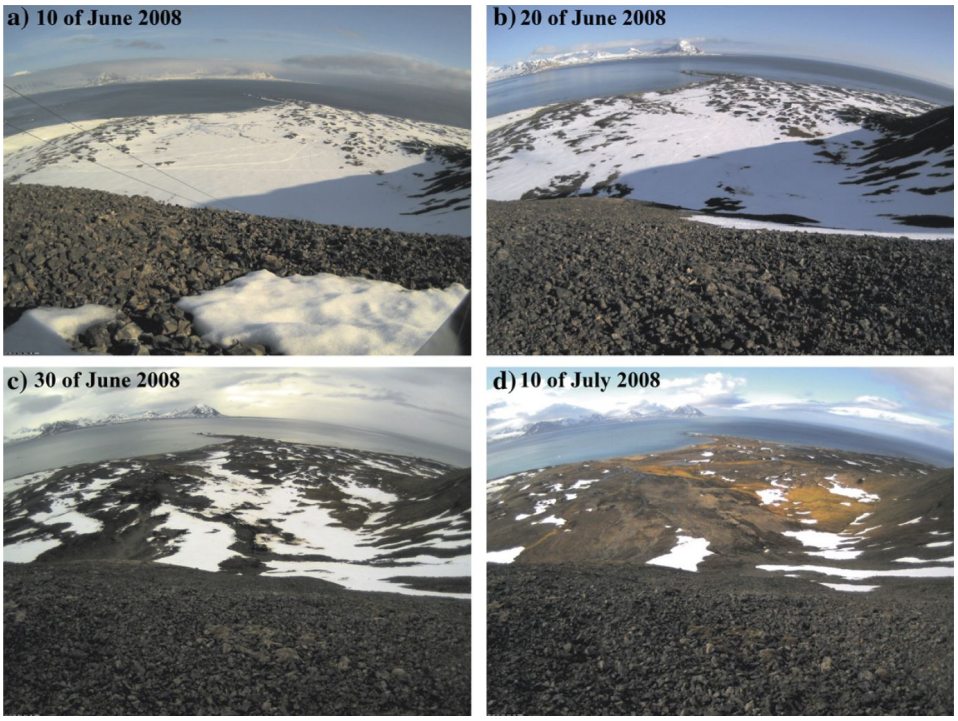

Figure 32: Progress of snow-melt process during summer months in a high-mountainous catchment: The photos were taken during summer months in a high-mountainous catchment in Spitsbergen. An important aspect hereby is the abundance of visible soils. Only d) shows some vegetation in lower zones. Pictures by Migała et al. (2014).

mainly right.

As can be seen from fig. 32, high mountainous zones show little vegetation due to the abundance of soils. Current study includes many catchments with elevation bands up to 3500 m and more, their snowpacks only melting during mid- to late summer months. Also pointing in that direction is a field study by Bales et al. (2011), in which the authors measured soil moisture in different soil depths in a "rain-snow transition catchment" of the southern Sierra Nevada. Despite the high elevation of 2000 m, the soils in their study are "wet and not frozen in winter, and dry out in the weeks following spring snowmelt and rain" (Bales et al. 2011, p. 786). They further state that "deep drainage" plays an important role, going up to 10 mm/d, which is exactly the process attempted to being described in current thesis. Therefore, the general approach of this thesis is considered to be correct in general, with the biggest uncertainty coming from the standard deviation of mean K values.

4.2 Efficiency of the snow model and discussion of missing factors

One of the major results of this thesis was to find simulated snowmelt rates to be 0.5 - 1 mm below mean rain rates when regarding all 78 catchments. But how sure can we be about this value, is it too low or maybe even not low enough? By validating our model through comparison with 8 SNOTEL sites, we could show that our simulated data has a MAE of 60 mm and the difference from modeled to measured snowdays would be 18 days for the whole wateryear in average. There is no sign for constant over- or underestimation of simulated snowpack, as results vary strongly between catchments. Cooley and Palmer (1997) did also examine snowmelt characteristics based on SNOTEL data. First, Cooley and Palmer's study is based on hourly resolution of snowmelt, telling

that there are huge differences between maximum daily declines in SWE and average daily declines of around 20 to 40 mm per day. These values are being backed by Rango and Martinec (1995), through the help of lysimeter outflow measurements.

Regarding my own study, probably the factor of maximum snowmelt per day is underestimated, which can easily reach the intensity of a strong rain event (e.g. 75 mm, Cooley and Palmer 1997). In terms of comparisons between snowmelt and rain, this is a general weakness of current study: As only dealing with data resolution on a daily basis, maximum events and the extended amount of snow/rain that is not able to infiltrate into bedrock during these events are ignored.

Again, Cooley and Palmer (1997) remind of the fact that evaporation as well as sublimation plays a role for snow influenced catchments, a factor that was completely missed out in this study's snow accounting approach. Bernhardt et al. (2012) modeled maximum hourly sublimation rates of 0.12 mm SWE, a value that is confirmed in its magnitude by other authors. Depending on the length of the snowmelt period, significant sublimation rates can be expected. MacDonald et al. (2010) found total sublimation to cumulative snowfall to be "20–32 % with the blowing snow sublimation loss amounting to 17–19 % of cumulative snowfall" (p. 1401). Strong snow sublimation is further contrary not only to my hypothesis but also to Berghuijs, Sivapalan, Woods and Savenije (2014)'s findings of higher streamflow being associated with a high snow factor. Bales et al. (2011) describe a total annual evapotranspiration value of 760 mm for the water-year 2009 in a Sierra Nevada catchment. These values show, that snow sublimation and evapotranspiration rates play a significant role in mountainous catchments. In terms of the results of current thesis, snowpack SWE and snowmelt are probably overestimated.

On the other hand, we implemented but didn't use the snow factor correction factor (SFCF) in our model, due to calibration results. By the help of this parameter, snowfall amounts would sometimes be extended up to 80 % of their original value, e.g. in Stahl et al. (2008). MOPEX precipitation data is already corrected to fit the catchment area, with no separation into rain and snow. Daily and hourly data sets from the National Climate Data Center (NCDC) are included as well as data from the SNOTEL network (Schaake et al. 2006). Therefore, MOPEX precipitation data can be considered exact and a SFCF is not of necessity.

The separation into rain and snow was realized with the exact same approach as in Berghuijs, Sivapalan, Woods and Savenije (2014), with a temperature threshold of 1°C. Therefore and also shown by the good NSE values (0.83) we assume that our modeled snowpack SWE is mainly correct. And finally, when regarding the SNOTEL data reference SWE, there is no absolute certainty for the reference data to be correct. As shown by Yang (2014), SWE measuring methods result in various over/underestimation schemes. Additionally, it was not possible to find a matching SNOTEL site inside every calibration catchment. A snowpack SWE bias to the modeled SWE is therefore more than plausible, resulting in a worse model efficiency .

4.3 The karst phenomenon as a subsidiary for regional small-scale patterns

To start off with this section, a single catchment shown in fig. 29 is recalled, showing a negative INF-NAS effect but a positive SIRI-NAS correlation. Is there a possible explanation for this obvious discrepancy for Wind River catchment near Crowheart, Wyoming? Or is the whole concept to be questioned by this? In fig. 33 a hint on possible disturbances regarding "normal" hydrogeo-

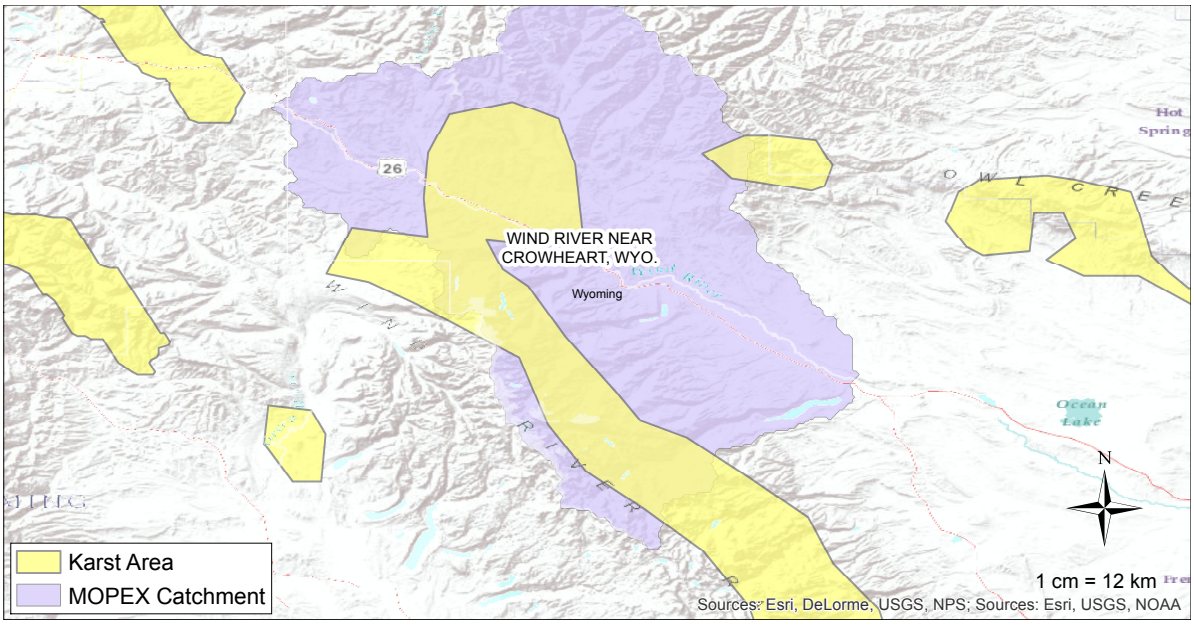

Figure 33: Karst influenced catchment "Wind River", Wyoming: Wide parts of the catchment are karst influenced, meaning that weathered limestone is the main geological structure unit. Depending on the development of the karst phenomenon, hydrological processes can be strongly influenced as karst is extremely permeable for infiltrating water in spots.

logical flow processes can be seen, as the catchment is strongly karst influenced. This means, that in parts of the catchment water can infiltrate almost without any resistance from the bedrock, as the underlying limestone is strongly weathered and has got large fissures and gaps. Karst aquifers are of high heterogeneity, created by groundwater flow, with high flow velocities in the dimension of several hundred meters per hour (Bakalowicz 2005). In karst-influenced catchments, infiltrated water does not necessarily contribute to streamflow, as seepage can lead over wide distances. Hydrogeologists therefore often use tracer studies to examine the underground pathways of water in those catchments. Ravbar et al. (2012) for example used multi-tracer tests with fluorescent tracers to examine different pathways of solute transport in a karst system in Slovenia. Their study showed that depending on rainfall intensities, different flow paths occur, resulting in complicated groundwater systems.

The described phenomenon could possibly be of strong influence in Wind River catchment, fig. 34 gives some hints in that direction. From the example water year 1999, a year with a mean areal precipitation above average, one can see that streamflow shows little to no effect to rain events. The only exception can be seen during main melting season during May and June: The snowpack on the upper elevation bands is melting with 5 to 10 mm/d, with additional rain events occurring. ROS can also play a role, as the model parameters show that 9 % of rain volume melts the equal amount of SWE. Streamflow follows the snowmelt trend into a first peak at the end of May, and a second peak during mid-June. It must be assumed that a combination of saturated soils and ROS events leads to high streamflow. When trying to produce recharge simulations of karst systems in Europe, Hartmann et al. 2015 (p. 1741) found "that current large-scale modeling approaches tend to significantly under-estimate recharge volumes" and that "presence of preferential flow paths enhances recharge". But as the exact link between groundwater recharge and streamflow in Wind

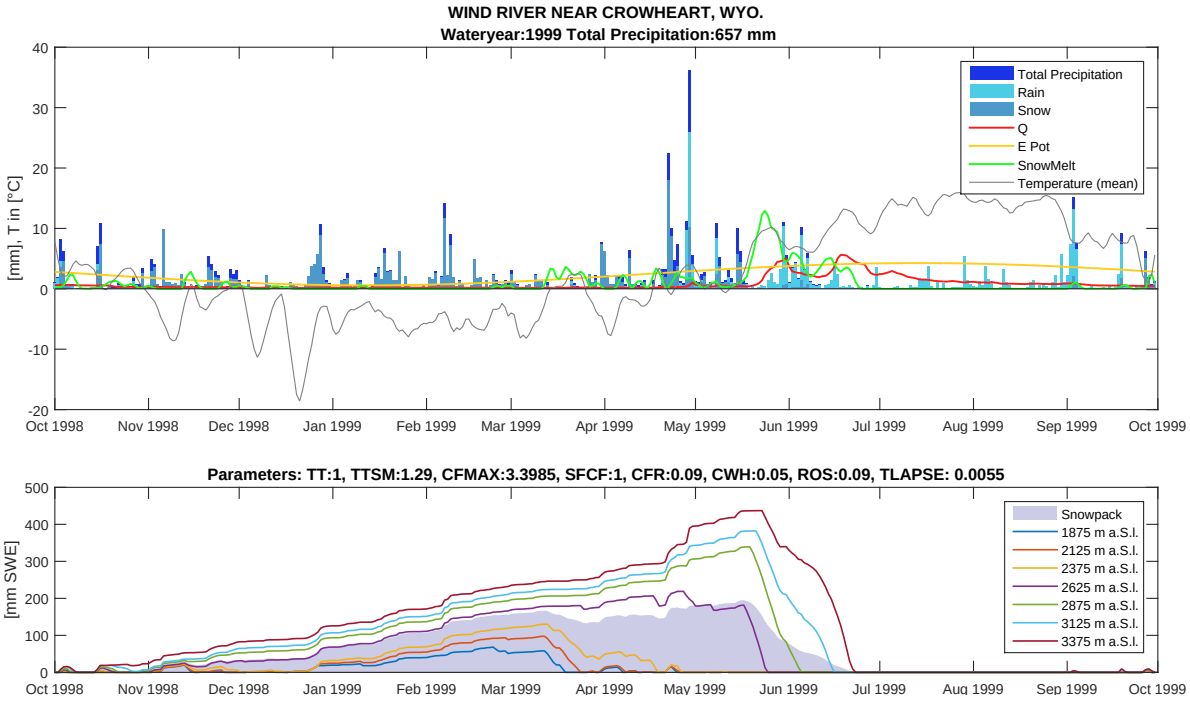

Figure 34: Example wateryear 1990 of karst-influenced catchment "Wind River": Precipitation of this year is above average, yet streamflow is little affected which is pointing to karst influence. The catchment's mean elevation is high-mountainous but larger snowpack amounts can only remain on the upper 4 elevation zones during summer. Parameters show that the catchment is part of DDF-zone 3 with the highest CFMAX of 3.4 mm/d °C.

River catchment is unknown, we are limited to observations resulting from modeled data here.

For the negative correlation between INF and NAS in this catchment, it's now understood that higher infiltration rates do not contribute to streamflow. The opposite is the case, the more surface runoff, the more streamflow. Additionally the results show, that a higher SIRI ratio leads to higher streamflow. This effect does not imply a contradiction here: With constantly high snowmelt rates during melting period, ROS events are likely to produce surface runoff, which directly contributes to streamflow (fig. 34).

Wind River catchment shows, how misleading large scale simulation and statistics can be, when small-scale regional processes are being neglected. Therefore, it must be admitted that the results of current thesis must be considered with caution, and further insight into every catchment has to be made before making general statements: Labat et al. (2000)(p.146) found karstic systems to be "non-linear and non-stationary", especially rainfall and corresponding streamflow rates "appear to be non-gaussian". This factor is extremely questioning the linear regression approach of current thesis. Karst effects like in Wind River catchment are not only being found in wide areas of the USA, but worldwide. And in various studies (e.g. Viles 2003, Hartmann et al. 2015) karstic systems are depicted to be of high vulnerability to climate change. Therefore, the current study's result is interesting, as one must assume that the positive effect of snowmelt influence on streamflow is going to be reduced by future climatic conditions.

5 Conclusion

A not entirely explained paper by Berghuijs, Sivapalan, Woods and Savenije (2014) was the primal idea of this thesis, stating that future climate conditions will result in lower annual streamflow due to less precipitation in the form of snow. The first goal of this thesis was to show, if daily snowmelt rates are lower than daily rain rates. Secondly in that case, hydraulic conductivity of bedrock as the main barrier for infiltrating water should be less limiting to snowmelt than to rain. This effect should therefore have a positive influence on streamflow. The hypothesis was intended to be substantiated by current work.

The efficient simulation of 53 years of daily snowmelt rates on a large scale for 78 catchments across the USA was demonstrated. These catchments, part of the MOPEX dataset, were chosen due to their snow factor of more than 15 % long-term ratio. The snow model was oriented according to HBV-SAR (Bergström 1976, Seibert 2010), with several modifications including ROS, a seasonal variable DDF and a 250 m height zone stepping. The DDF, as being hard to determine from literature, was clustered into 3 zones according to catchment mean elevation, slope and latitude. Calibration of model parameters as well as validation was done by the help of 18 years of SNOTEL reference SWE data for 8 of the 78 catchments. During calibration period (1984-1992), mean MAE was 56 mm with a NSE of 0.83. Mean MAE for all catchments during validation period (1993-2001) was 60 mm, with a NSE of 0.83 again. The total difference of simulated to reference days with snowpack was 16 days for the calibration period and 18 days for the validation period. The modeled snowpack and snowmelt rates were additionally visually controlled by random tests. Various control routines were implemented, e.g. an incomplete melting of a years snowpack leads to exclusion from the data set.

When analyzing modeled snowmelt rates, it was shown that differences between catchments are massive, depending mostly on special characteristics during snowmelt period: Some catchments contribute to streamflow via snowmelt over half a hear. Others loose the entire snowpack in under 2 months. Further processes influencing snowmelt rates are the general extent of the snowpack and the season, during which main snowmelt takes place. With the DDF strongly depending on temperature, quick temperature rises during summer are able to release large amounts of SWE from the snowpack. Melting rates of more than 50 mm SWE per day are possible, but in most catchments only the upper elevation bands maintain their snowpack until summer. This factor is of high importance regarding climate change, as vegetation relies on streamflow fed mostly by snowmelt during these months. This effect could be observed frequently in the catchments with continental climate influence.

Furthermore, transregional inter-year patterns in mean snowmelt rates were visualized by the help of a pseudocolor plot. Mean daily snowmelt rates per catchment were found to be ranging between 2 and 8 mm/d, reaching up to 40 mm/d in extreme sites. By comparing daily snowmelt rates with daily rain data, it was shown that for most catchments mean rain rates are of higher intensity.

Mean catchment-wise hydraulic conductivities were computed via geometric mean, due to uneven distribution of occurring input bedrock permeability. Input data with bedrock permeability information was taken from the GlHyMps project by Gleeson et al. (2014). Standard deviation of original permeability data was processed by the Gauss'ian propagation of uncertainty calculation.

It was a main assumption of this thesis to regard bedrock conductivities as the only barrier for infiltration, soils were neglected. Mean hydraulic conductivities of the 78 catchments ranged in the magnitude of 2-10 mm/d. Extreme values were found to be around 0.5 mm/d at the lower and above 150 mm/d at the upper range. The amount of "blocked" water during infiltration process varied between catchments, with mean values of 20 % to 80 %. As expected, snowmelt turned out to being blocked less than rain. This pattern was not proven to be valid for all catchments, due to the catchments with extremely high or low K-values. Standard deviations of K typically were around 25 to 50 % of the original value, a factor that adds substantial uncertainty to the previous findings.

By the help of linear regressions and a SEM-approach to avoid auto-korrelation, annual streamflow of 50 % of the catchments was shown to be depending on infiltration rates. Furthermore, it was revealed that a strong annual snowmelt component in infiltration composition is correlating with annual higher streamflow in 25 % of the 78 catchments.

When discussing the results, the initial approach of permanent saturated soils was criticized, as soils depict an important buffer for water and can therefore result in delayed streamflow response to snowmelt processes. Yet it could be shown that bedrock is the stronger limitation than soil in most cases and that soils are often little developed in high-mountainous areas. Most importantly, this study only dealt with streamflow as an annual sum and not with the processes of snowmelt and direct streamflow response.

Further criticism to the modeling approach results from the missing integration of total evapotranspiration and snow sublimation. Literature study showed that these factors play an important role in snow hydrology, but are not easily being quantified. Future studies into the field of snowmelt, bedrock conductivity and streamflow should therefore include the previously named defects.

Small scale processes were being discussed on the basis of a catchment with karst influence. The example showed that the obvious discrepancy for this catchment as derived from the results could be mitigated, by taking a closer look on the underlying processes. Therefore, regarding correlation between infiltration and streamflow, some results tend to be misleading as long as a closer look on regional processes is neglected. As a result, the simulated snowmelt rates and their evaluation in this thesis are only good in terms of depicting trends on a large scale.

The results of current study were partly able to confirm the original hypothesis. The concept of bedrock as a barrier is valid, as long as soils are being neglected. Extended groundwater recharge has a positive effect on streamflow in 50 % of all catchments of this study. Snowmelt plays a role in terms of infiltration capacities, but only a quarter of all catchments was found to be positively influenced by this effect.

As can be said from the results of this study, climate change will have a strong impact on snow influenced catchments: Streamflow will decrease as a result of less snowmelt infiltration. And most importantly for vegetation, there will be a shift and shortening of the snowmelt period. The results of this study must not be overrated, as small scale effects on catchment level were being neglected. But convincing field studies and further improved modeling approaches could substantiate the general trend, set by the results of this thesis.

References

Bakalowicz, M.: 2005, Karst groundwater: A challenge for new resources, *Hydrogeology Journal* **13**(1), 148–160.

Bales, R. C., Hopmans, J. W., O'Geen, A. T., Meadows, M., Hartsough, P. C., Kirchner, P., Hunsaker, C. T. and Beaudette, D.: 2011, Soil moisture response to snowmelt and rainfall in a sierra nevada mixed-conifer forest, *Vadose Zone Journal* **10**(3), 786.

Barnett, T. P., Adam, J. C. and Lettenmaier, D. P.: 2005, Potential impacts of a warming climate on water availability in snow-dominated regions, *Nature* **438**(7066), 303–309.

Barnett, T. P. and Pennell, W.: 2004, Impact of global warming on western us water supplies, *Clim. Change* **62**.

Bavay, M., Lehning, M., Jonas, T. and Löwe, H.: 2009, Simulations of future snow cover and discharge in alpine headwater catchments, *Hydrological Processes* **23**(1), 95–108.

Berghuijs, W. R., Sivapalan, M., Woods, R. A. and Savenije, H. H. G.: 2014, Patterns of similarity of seasonal water balances: A window into streamflow variability over a range of time scales, *Water Resources Research* **50**(7), 5638–5661.

Berghuijs, W. R., Woods, R. A. and Hrachowitz, M.: 2014a, A precipitation shift from snow towards rain leads to a decrease in streamflow, *Nature Climate Change* **4**(7), 583–586.

Berghuijs, Woods and Hrachowitz: 2014b, Supplementary material: A precipitation shift from snow towards rain leads to a decrease in streamflow: Supplementary information, *Nature Climate Change* **4**(7), 583–586.

Bergström, S.: 1976, *Development and application of a conceptual runoff model for Scandinavian catchments: SMHI RHO 7.*, Norrköping.

Bernhardt, M., Schulz, K., Liston, G. E. and Zängl, G.: 2012, The influence of lateral snow redistribution processes on snow melt and sublimation in alpine regions, *Journal of Hydrology* **424-425**, 196–206.

Brown, R. D. and Mote, P. W.: 2009, The response of northern hemisphere snow cover to a changing climate*, *Journal of Climate* **22**(8), 2124–2145.

Campbell, J. L., Ollinger, S. V., Flerchinger, G. N., Wicklein, H., Hayhoe, K. and Bailey, A. S.: 2010, Past and projected future changes in snowpack and soil frost at the hubbard brook experimental forest, new hampshire, usa, *Hydrological Processes* pp. n/a–n/a.

Cooley, K. R. and Palmer, P. (eds): 1997, *Characteristics of snowmelt from NRCS SNOTEL (SNOwTELemetry) sites*, Vol. 65, Colorado State University.

Daly, C., Neilson, R. P. and Phillips, D. L.: 1994, A statistical-topographic model for mapping climatological precipitation over mountainous terrain, *Journal of Applied Meteorology* **33**(2), 140–158.

Dormann, C. F.: 2013, *Parametrische Statistik: Verteilungen, maximum likelihood und GLM in R*, SpringerLink : Bücher, Springer Spektrum, Berlin, Heidelberg.

Duan, Q., Schaake, J., Andréassian, V., Franks, S., Goteti, G., Gupta, H. V., Gusev, Y. M., Habets, F., Hall, A., Hay, L., Hogue, T., Huang, M., Leavesley, G., Liang, X., Nasonova, O. N., Noilhan, J., Oudin, L., Sorooshian, S., Wagener, T. and Wood, E. F.: 2006, Model parameter estimation experiment (mopex): An overview of science strategy and major results from the second and third workshops, *Journal of Hydrology* **320**(1-2), 3–17.

Finger, D., Vis, M., Huss, M. and Seibert, J.: 2015, The value of multiple data set calibration versus model complexity for improving the performance of hydrological models in mountain catchments, *Water Resources Research* **51**(4), 1939–1958.

Freudiger, D., Kohn, I., Stahl, K. and Weiler, M.: 2014, Large-scale analysis of changing frequencies of rain-on-snow events with flood-generation potential, *Hydrology and Earth System Sciences* **18**(7), 2695–2709.

Garvelmann, J., Pohl, S. and Weiler, M.: 2015, Spatio-temporal controls of snowmelt and runoff generation during rain-on-snow events in a mid-latitude mountain catchment, *Hydrological Processes* **29**(17), 3649–3664.

Gburek, W. J. and Folmar, G. J.: 1999, A groundwater recharge field study: Site characterization and initial results, *Hydrological Processes* **13**(17), 2813–2831.

Gleeson, T., Moosdorf, N., Hartmann, J. and van Beek, L. P. H.: 2014, A glimpse beneath earth's surface: Global hydrogeology maps (glhymps) of permeability and porosity, *Geophysical Research Letters* **41**(11), 3891–3898.

Gleeson, T., Novakowski, K. and Kurt Kyser, T.: 2009, Extremely rapid and localized recharge to a fractured rock aquifer, *Journal of Hydrology* **376**(3-4), 496–509.

Gleeson, T., Smith, L., Moosdorf, N., Hartmann, J., Dürr, H. H., Manning, A. H., van Beek, Ludovicus P. H. and Jellinek, A. M.: 2011, Mapping permeability over the surface of the earth, *Geophysical Research Letters* **38**(2), n/a–n/a.

Grace, J. B., Scheiner, S. M. and Schoolmaster Jr, D. R.: 2015, Structural equation modeling: building and evaluating causal models: Chapter 8.

Hartmann, A., Gleeson, T., Rosolem, R., Pianosi, F., Wada, Y. and Wagener, T.: 2015, A large-scale simulation model to assess karstic groundwater recharge over europe and the mediterranean, *Geoscientific Model Development* **8**(6), 1729–1746.

Hock, R.: 2003, Temperature index melt modelling in mountain areas, *Journal of Hydrology* **282**(1-4), 104–115.

Hölting, B. and Coldewey, W. G.: 2009, *Hydrogeologie: Einführung in die allgemeine und angewandte Hydrogeologie ; 90 Tabellen*, 7., neu bearb. und erw. aufl. edn, Spektrum Akad. Verl., Heidelberg.

Isard, S. A. and Schaetzl, R. J.: 1998, Effects of winter weather conditions on soil freezing in southern michigan, *Physical Geography* **19**(1), 71–94.

J.E. Nash and J.V. Sutcliffe: 1970, River flow forecasting through conceptual models part i — a discussion of principles, *Journal of Hydrology* **10**(3), 282–290.
URL: *http://www.sciencedirect.com/science/article/pii/0022169470902556*

Labat, D., Ababou, R. and Mangin, A.: 2000, Rainfall–runoff relations for karstic springs. part i: Convolution and spectral analyses, *Journal of Hydrology* **238**(3-4), 123–148.

Lindström, G. and Bergstöm, S.: 1992, Improving the hbv and pulse-models by use of temperature anomalies, *Vannet i Norden* (1), 16–23.

MacDonald, M. K., Pomeroy, J. W. and Pietroniro, A.: 2010, On the importance of sublimation to an alpine snow mass balance in the canadian rocky mountains, *Hydrology and Earth System Sciences* **14**(7), 1401–1415.

Macpherson, G. and Sophocleous, M.: 2004, Fast ground-water mixing and basal recharge in an unconfined, alluvial aquifer, konza lter site, northeastern kansas, *Journal of Hydrology* **286**(1-4), 271–299.

Marks, D., Kimball, J., Tingey, D. and Link, T.: 1998, The sensitivity of snowmelt processes to climate conditions and forest cover during rain-on-snow: a case study of the 1996 pacific northwest flood, *HYDROLOGICAL PROCESSES* **12**(10-11), 1569–1587.

McCabe, G. J., Hay, L. E. and Clark, M. P.: 2007, Rain-on-snow events in the western united states, *Bulletin of the American Meteorological Society* **88**(3), 319–328.

Migała, K., Wojtuń, B., Szymański, W. and Muskała, P.: 2014, Soil moisture and temperature variation under different types of tundra vegetation during the growing season: A case study from the fuglebekken catchment, sw spitsbergen, *CATENA* **116**, 10–18.

Nolin, A. W., Phillippe, J., Jefferson, A. and Lewis, S. L.: 2010, Present-day and future contributions of glacier runoff to summertime flows in a pacific northwest watershed: Implications for water resources, *Water Resources Research* **46**(12), n/a–n/a.

NRCS: 2008, A measure of snow: A report based on case studies of a report based on case studies of the snow survey and water supply forecasting program.
URL: *http://www.wcc.nrcs.usda.gov/publications/factsheets.html*

Ostendorf, D. W., Lukas, W. G. and Rotaru, C.: 2015, Recharge and pumping hydraulics in a till drumlin above fractured bedrock (massachusetts, usa), *Hydrogeology Journal* **23**(4), 741–756.

Pellicciotti, F., Brock, B., Strasser, U., Burlando, P., Funk, M. and Corripio, J.: 2005, An enhanced temperature-index glacier melt model including the shortwave radiation balance: Development and testing for haut glacier d'arolla, switzerland, *Journal of Glaciology* **51**(175), 573–587.

Pomeroy, J. W., Bewley, D. S., Essery, R. L. H., Hedstrom, N. R., Link, T., Granger, R. J., Sicart, J. E., Ellis, C. R. and Janowicz, J. R.: 2006, Shrub tundra snowmelt, *Hydrological Processes* **20**(4), 923–941.

Pomeroy, J. W., Gray, D. M., Brown, T., Hedstrom, N. R., Quinton, W. L., Granger, R. J. and Carey, S. K.: 2007, The cold regions hydrological model: A platform for basing process representation and model structure on physical evidence, *Hydrological Processes* **21**(19), 2650–2667.

Rango, A. and Martinec, J.: 1995, Revisiting the degree-day method for snowmelt computations, *Journal of the American Water Resources Association* **31**(4), 657–669.

Rasouli, K., Pomeroy, J. W., Janowicz, J. R., Carey, S. K. and Williams, T. J.: 2014, Hydrological sensitivity of a northern mountain basin to climate change, *Hydrological Processes* **28**(14), 4191–4208.

Ravbar, N., Barberá, J. A., Petrič, M., Kogovšek, J. and Andreo, B.: 2012, The study of hydrodynamic behaviour of a complex karst system under low-flow conditions using natural and artificial tracers (the catchment of the unica river, sw slovenia), *Environmental Earth Sciences* **65**(8), 2259–2272.

Rodhe, A. and Bockgård, N.: 2006, Groundwater recharge in a hard rock aquifer: A conceptual model including surface-loading effects, *Journal of Hydrology* **330**(3-4), 389–401.

Schaake, J. C., Cong and S., Q. D.: 2006, U.s. mopex data set: Data set description.

Schmucki, E., Marty, C., Fierz, C. and Lehning, M.: 2014, Evaluation of modelled snow depth and snow water equivalent at three contrasting sites in switzerland using snowpack simulations driven by different meteorological data input, *Cold Regions Science and Technology* **99**, 27–37.

Seibert, J.: 1997, Estimation of parameter uncertainty in the hbv model, *NORDIC HYDROLOGY* **28**(4-5), 247–262.

Seibert, J.: 2010, Hbv-help: Manual to hbv gui v. 3.0.0.1.

Seyfried, M. S., Grant, L. E., Marks, D., Winstral, A. and McNamara, J.: 2009, Simulated soil water storage effects on streamflow generation in a mountainous snowmelt environment, idaho, usa, *Hydrological Processes* **23**(6), 858–873.

Singh, P. and Bengtsson, L.: 2004, Hydrological sensitivity of a large himalayan basin to climate change, *Hydrological Processes* **18**(13), 2363–2385.

Stahl, K., Moore, R. D., Floyer, J. A., Asplin, M. G. and McKendry, I. G.: 2006, Comparison of approaches for spatial interpolation of daily air temperature in a large region with complex topography and highly variable station density, *Agricultural and Forest Meteorology* **139**(3-4), 224–236.

Stahl, K., Moore, R. D., Shea, J. M., Hutchinson, D. and Cannon, A. J.: 2008, Coupled modelling of glacier and streamflow response to future climate scenarios, *Water Resources Research* **44**(2).

Stewart, I. T., Cayan, D. R. and Dettinger, M. D.: 2005, Changes toward earlier streamflow timing across western north america, *Journal of Climate* **18**(8), 1136–1155.

Stottlemyer, R. and Toczydlowski, D.: 1991, Stream chemistry and hydrologic pathways during snowmelt in a small watershed adjacent lake superior, *Biogeochemistry* **13**(3).

Stottlemyer, R. and Toczydlowski, D.: 1999, Seasonal change in precipitation, snowpack, snowmelt, soil water and streamwater chemistry, northern michigan, *Hydrological Processes* **13**(14-15), 2215–2231.

USDA: 2014, Brochure: Snotel and snow survey & water supply forecasting: Helping people help the land.

Valéry, A., Andréassian, V. and Perrin, C.: 2014, 'as simple as possible but not simpler': What is useful in a temperature-based snow-accounting routine? part 2 – sensitivity analysis of the cemaneige snow accounting routine on 380 catchments, *Journal of Hydrology* **517**, 1176–1187.

Viles, H. A.: 2003, Conceptual modeling of the impacts of climate change on karst geomorphology in the uk and ireland, *Journal for Nature Conservation* **11**(1), 59–66.

Voeckler, H. and Allen, D. M.: 2012, Estimating regional-scale fractured bedrock hydraulic conductivity using discrete fracture network (dfn) modeling, *Hydrogeology Journal* **20**(6), 1081–1100.

Winstral, A., Marks, D. and Gurney, R.: 2014, Assessing the sensitivities of a distributed snow model to forcing data resolution, *Journal of Hydrometeorology* **15**(4), 1366–1383.

Yang, D.: 2014, Double fence intercomparison reference (dfir) vs. bush gauge for "true" snowfall measurement, *Journal of Hydrology* **509**, 94–100.

Zinn, B. and Harvey, C. F.: 2003, When good statistical models of aquifer heterogeneity go bad: A comparison of flow, dispersion, and mass transfer in connected and multivariate gaussian hydraulic conductivity fields, *Water Resources Research* **39**(3), n/a–n/a.

Appendix

Table A.1: Overview of MATLAB data preparation routines

Routine	Purpose
Import_6h-Precip_and_Temperature.m	Import MOPEX files, deal with units and date
Delete_Catchments_With_Large_Data_Gaps.m	Handle NaN-values, delete all catchments with less than 15 years of data
Snow_Factor_Budyko_HBV.m	This script Takes all 423 MoPex Catchments. It tests if snow the factor is above 15 % and stores all positive ones in new matfile 'Snow_Influenced_96'. Additionally, one can apply the Budyko framework on data and test if similar plots as in Berghuijs, Woods and Hrachowitz (2014b) are possible
SnowAffectedData.m	Compute test values for all catchments, export results to GIS for visual control
NO_Nested_Hydrological_Year	Compute final data set without nested catchments and formatted in hydrological years

Table A.2: Overview of MATLAB snow model routines

Routine	Purpose
Snotel_Data_Unify.m	open import SNOTEL data and prepare for calibration
Monte_Carlo_Sim.m	Monte Carlo routine
Snow_Routine_Final.m	encapsulated snow routine, called by Main_routine_MC and Main_routine
validation.m	encapsulated validation routine, calculates MAE, MSD, NSE etc.
Main_routine.m	final simulation routine
Main_routine_val_test.m	control routine, plots catchments with SNOTEL reference
Main_routine_only_val.m	validation of selected years
Solo_SR_plot_part.m	encapsulated plot routine, called by Main_routine.m
Plot_single_catchment	control plot of any simulated catchment and year

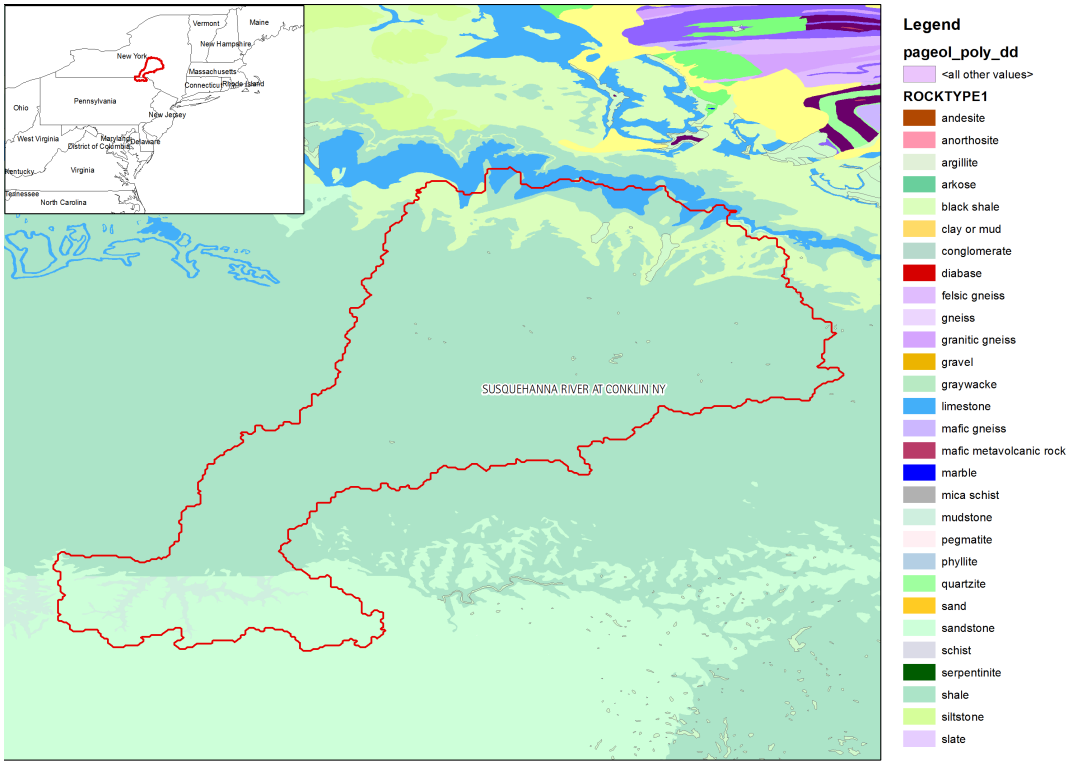

Figure A.1: Geology of Susquehanna River catchment: Although many different colors are visible, the catchment's geology itself is quite homogeneous, built of mostly sedimentary rock types. Geology at the Northern border of the catchment is more heterogeneous, with limestone as the predominant rock type.

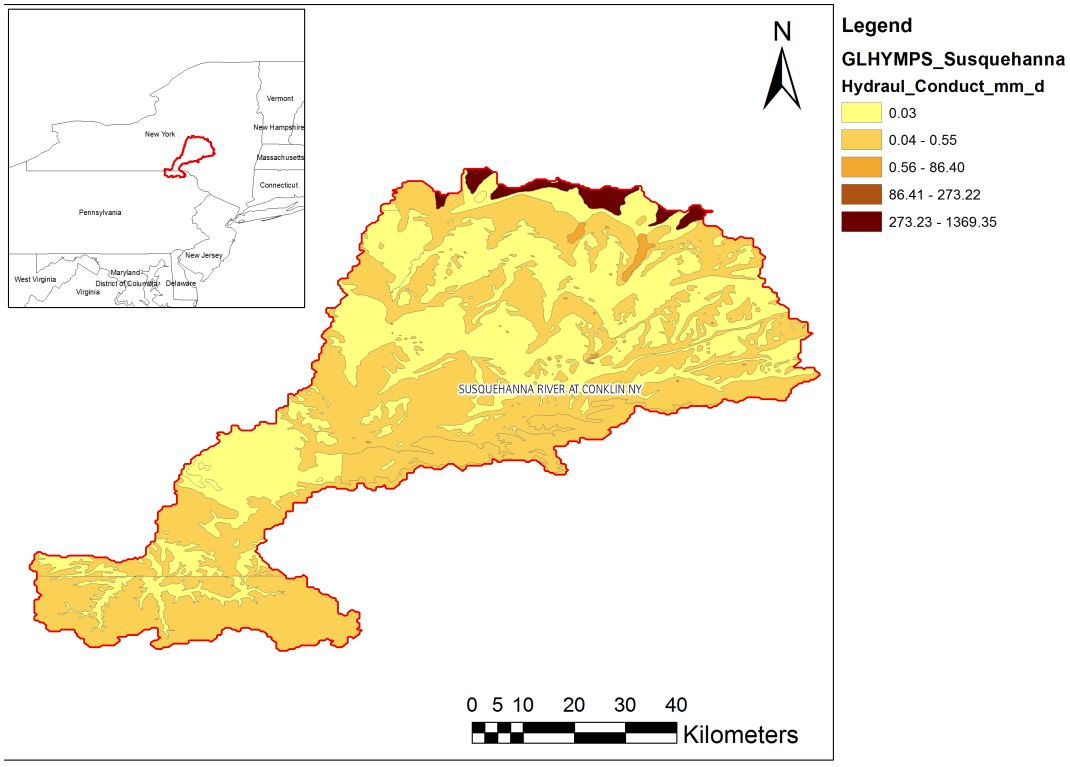

Figure A.2: Hydraulic conductivity K of Susquehanna River catchment: K is depicted in mm/d. The catchment is a good example for the uneven distribution of K-values: Predominant are low K-values with small areas of very high K-values.

Table A.3: Overview of MATLAB analysis routines

Routine	Purpose
Analysis_GeoMean.m	Main routine to call simulated data and apply the statistical analysis preparation
Effect_P_Q.m	SEM: Testing correlation between P and Q
Effect_P_Inf.m	SEM: Testing correlation between P and INF
Effect_P_SIRI.m	SEM: Testing correlation between P and SIRI
Corr_INF_Q.m	Correlation between INF and Q, uses output from SEM routines;
Corr_SIRI_Q.m	Correlation between SIRI and Q, uses output from SEM routines;
Plot_Single_Catchment_funktion.m	Plot function, Called by (Catchment, Year, SimulationType, ParameterSet)
SaveTightFigure.m	Help routine to get rid of white margins around plots
Thesis_Plots.m	Prepare final plots for thesis, output as PDF-file (vectorized)

Ehrenwörtliche Erklärung

Hiermit erkläre ich, dass die Arbeit selbständig und nur unter Verwendung der angegebenen Hilfsmittel angefertigt wurde.

Ort, Datum Unterschrift